



UNIVERSITY
IYUNIVESITHI
UNIVERSITEIT

E344 Assignment 1

Gary Allen

23905093

Report submitted in partial fulfilment of the requirements of the module
Design (E) 344 for the degree Baccalaureus in Engineering in the Department of Electrical
and Electronic Engineering at Stellenbosch University.

September 29, 2022

Plagiaatverklaring / Plagiarism Declaration

1. Plagiaat is die oorneem en gebruik van die idees, materiaal en ander intellektuele eiendom van ander persone asof dit jou eie werk is.

Plagiarism is the use of ideas, material and other intellectual property of another's work and to present is as my own.

2. Ek erken dat die pleeg van plagiaat 'n strafbare oortreding is aangesien dit 'n vorm van diefstal is.

I agree that plagiarism is a punishable offence because it constitutes theft.

3. Ek verstaan ook dat direkte vertalings plagiaat is.

I also understand that direct translations are plagiarism.

4. Dienooreenkomsdig is alle aanhalings en bydraes vanuit enige bron (ingesluit die internet) volledig verwys (erken). Ek erken dat die woordelikse aanhaal van teks sonder aanhalingsstekens (selfs al word die bron volledig erken) plagiaat is.

Accordingly all quotations and contributions from any source whatsoever (including the internet) have been cited fully. I understand that the reproduction of text without quotation marks (even when the source is cited) is plagiarism

5. Ek verklaar dat die werk in hierdie skryfstuk vervat, behalwe waar anders aangedui, my eie oorspronklike werk is en dat ek dit nie vantevore in die geheel of gedeeltelik ingehandig het vir bepunting in hierdie module/werkstuk of 'n ander module/werkstuk nie.

I declare that the work contained in this assignment, except where otherwise stated, is my original work and that I have not previously (in its entirety or in part) submitted it for grading in this module/assignment or another module/assignment.

23905093	
Studentenommer / Student number	Handtekening / Signature
G. Allen Voorletters en van / Initials and surname	September 29, 2022 Datum / Date

Contents

Declaration	i
List of Figures	v
List of Tables	viii
Nomenclature	ix
1. Literature Review	1
1.1. Operational Amplifiers	1
1.1.1. Basic Principles	1
1.1.2. Limitations	1
1.1.3. Key Specifications	2
1.1.4. Configurations	2
1.2. Current Sensing	3
1.2.1. Techniques	3
1.2.2. High-Side vs Low-Side	3
1.2.3. AC, DC and Power Requirements	3
1.3. Ultrasonic Sensors	4
1.3.1. Interfacing with the Range Sensor	4
1.3.2. Fundamental Operation of Range Sensors	5
1.4. PWM to Analog Conversion	6
1.5. Digital to Analog Conversion	7
1.5.1. Configurations	7
1.5.2. Impedance Requirements	7
1.6. Lead-Acid Batteries	8
2. Detailed Design	9
2.1. System Design	9
2.2. Voltage Regulation	10
2.3. Current Sensor	11
2.3.1. Configuration	11
2.3.2. Gain	11
2.3.3. Filter	11
2.3.4. Design	12
2.3.5. Circuit Diagram	12
2.4. Ultrasonic Sensor	13

2.4.1.	Power and Output Requirements	13
2.4.2.	Filter Selection	13
2.4.3.	Configuration	13
2.4.4.	Gain Stage	14
2.4.5.	Filter Stage	14
2.5.	Digital to Analog Converter	15
2.5.1.	Configuration and Impedance Requirements	15
2.5.2.	Summing Stage	15
2.6.	Analog Motor Controller	16
2.6.1.	Configuration	16
2.6.2.	Power Stage	16
2.6.3.	Subtractor Stage	16
2.7.	Digital Motor Controller: Firmware	18
2.7.1.	Flow Diagrams	18
2.7.2.	Range Measurement	18
2.7.3.	PWM Control	18
2.8.	Digital Motor Controller: Switch and Current Sensor	19
2.8.1.	Configuration	19
2.8.2.	Input Resistors	19
2.8.3.	Transistor Requirements	19
2.8.4.	Current Sensor	20
2.8.5.	Circuit Diagram	20
2.9.	Battery Charger	21
2.9.1.	Configuration	21
2.9.2.	Voltage and Current Considerations	21
2.9.3.	Design	21
2.10.	Battery Reader	22
2.10.1.	Configuration	22
2.10.2.	Input and Output Range	22
2.10.3.	Design	23
2.11.	Under-Voltage Protection	23
2.11.1.	Configuration	23
2.11.2.	Input Range	24
2.11.3.	Design	24
2.12.	Serial Communication	25
2.12.1.	Protocol	25
3.	Results	26
3.1.	Voltage Regulation	26
3.1.1.	Measured	26

3.2. Current Sensor	27
3.2.1. Simulated	27
3.2.2. Measured	27
3.3. Range Sensor	29
3.3.1. Simulated	29
3.3.2. Measured	30
3.4. Digital to Analog Converter	31
3.4.1. Simulated	31
3.4.2. Measured	31
3.5. Analog Motor Controller	32
3.5.1. Simulated	32
3.5.2. Measured	33
3.6. Digital Motor Controller	34
3.6.1. Simulated	34
3.6.2. Measured	35
3.7. Battery Charger	36
3.7.1. Simulated	36
3.7.2. Measured	37
3.8. Battery Reader and Under-Voltage Protection	38
3.8.1. Simulated	38
3.8.2. Measured	39
4. Physical Implementation	40
4.1. Combined Circuit	40
4.2. Current Sensor	41
4.3. Range Sensor	42
4.4. Digital to Analog Converter	43
Bibliography	44
A. Social contract	47
B. GitHub Activity Heatmap	48
C. Formulae and Derivations	49
C.1. Filters	49
C.1.1. Common Filter Formulae	49
C.1.2. 2 nd Order Filter Attenuation	49
C.1.3. 1 st and 2 nd Order Filter Cutoff vs Attenuation	50

List of Figures

1.1.	Non-Inverting Amplifier [5]	2
1.2.	Modified Non-Inverting Amplifier [6]	2
1.3.	Differential Amplifier [5]	2
1.4.	Instrumentation Amplifier [5]	2
1.5.	Hall Effect Sensor Working Principle [9]	3
1.6.	TTL Input/Output Levels [10]	4
1.7.	Sensor Timing Diagram [3]	4
1.8.	Simple Ultrasonic Sensing System [20]	5
1.9.	PWM Signal Voltage vs Time [11]	6
1.10.	Filtered PWM Signal [12]	6
1.11.	Non-Inverting Mode with Resistor-Weighted Network [22]	7
1.12.	Inverting Mode with R2R Ladder Network [23]	7
1.13.	The 3 Charging Stages for Lead-Acid Batteries	8
2.1.	Final System Block Diagram	9
2.2.	3.3 V Circuit [27]	10
2.3.	5 V Circuit [27]	10
2.4.	Current Sensor Circuit Diagram	12
2.5.	Range Sensor Amplifier Circuit Diagram	14
2.6.	Digital to Analog Converter Circuit Diagram	15
2.7.	Motor Controller Subtractor Stage Circuit Diagram	17
2.8.	Motor Controller Power Stage Circuit Diagram	17
2.9.	Setup Diagram	18
2.10.	Echo Interrupt Diagram	18
2.11.	Loop Diagram	18
2.12.	Digital Motor Controller and Current Sensor Circuit Diagram	20
2.13.	Battery Charger Circuit Diagram	22
2.14.	Battery Reader Circuit Diagram	22
2.15.	Under-Voltage Protection Circuit Diagram	23
3.1.	3.3 V Regulator Ripple Measurement	26
3.2.	5 V Regulator Ripple Measurement	26
3.3.	Output and Noise Level in Response to Step Input	27
3.4.	Current Draw	27
3.5.	Noise Level	28
3.6.	Step Response	28

3.7. Open Circuit to Free Running	28
3.8. Increasing Load	28
3.9. Free Running to Stall	28
3.10. Full-Range PWM using Modified Workbench	29
3.11. 400 mV Step Response Input vs Output	29
3.12. Noise Level	29
3.13. Current Draw	29
3.14. Noise Level	30
3.15. Step Response	30
3.16. Gradual Change over Input Range	30
3.17. Output Range from 0000 (First Cursor) to 1111 (Second Cursor)	31
3.18. Current Draw (Amplifier and Digital Inputs)	31
3.19. DAC Output at 0000	31
3.20. DAC Output at 0001	31
3.21. DAC Output at 1110	31
3.22. DAC Output at 1111	31
3.23. Motor Controller Output of Subtractor Stage	32
3.24. Motor Controller Current Draw of Subtractor Stage	32
3.25. Motor Controller Output of Power Stage	32
3.26. Motor Voltage: Object Far, Speed 0000	33
3.27. Motor Voltage: Object Far, Speed 1111	33
3.28. Motor Voltage: Object Near, Speed 0000	33
3.29. Motor Voltage: Object Near, Speed 1111	33
3.30. Motor Voltage: Object 20cm, Speed 1111	33
3.31. Motor Output Voltage vs Motor Control	34
3.32. Motor Current vs Current Sensor Output	34
3.33. MOSFET Turn On Time vs Motor Control	34
3.34. Object Far, DAC 1111	35
3.35. Object Far, DAC 0000	35
3.36. Object Near, DAC 1111	35
3.37. Object Near, DAC 0000	35
3.38. Object 50cm, DAC 1111	35
3.39. Batter Charger Final Voltage and Current	36
3.40. Battery Charger Internal Voltage Regulation vs Changing Load	36
3.41. Battery Charger No-Load Voltage	37
3.42. Battery Charger Voltage with 1 k Ω Load	37
3.43. Battery Charger Voltage with 50 Ω Load	37
3.44. Battery Charger with 15 Ω Load (approx. uncharged battery)	37
3.45. Battery Charger Voltage Regulation under Changing Load	37
3.46. Battery Reader Output vs 5.0 to 7.2 V Input	38

3.47. Under-Voltage Schmitt Trigger Output vs Sine Wave Input	38
3.48. Battery Reader at 7.2V	39
3.49. Battery Reader at 5.9V	39
3.50. Battery Reader at 5.9V with Under-Voltage Protection Battery Voltage	39
3.51. Under-Voltage Protection Output of Schmitt Trigger	39
3.52. Under-Voltage Protection Output of Battery Voltage	39
4.1. Final Combined Circuit	40
4.2. Current Sensor Physical Circuit	41
4.3. Ultrasonics Sensor Amplifier Physical Circuit	42
4.4. Digital to Analog Converter Physical Circuit	43

List of Tables

1.1.	Input Impedance of Various Summing Configurations	7
2.1.	Filter type vs Rise Time and Attenuation using [C.1.1]	13
2.2.	Output Conditions for Various Range and Sensor Inputs	17
2.3.	25
3.1.	Measurements of Motor Current and Voltage	28

Nomenclature

Variables and functions

V_{ss} Voltage positive.

V_{dd} Voltage negative.

Acronyms and abbreviations

CMRR	Common Mode Rejection Ratio
GBWP	Gain-Bandwidth Product
RC	Resistor-Capacitor
PWM	Pulse Width Modulation
LPF	Low Pass Filter
HPF	High Pass Filter
TTL	Transistor-Transistor Logic
MCU	Microcontroller Unit
ADC	Analog to Digital Converter
DAC	Digital to Analog Converter
AFE	Analog Front End
DSP	Digital Signal Processor
R2R	Resistor-2-Resistor
RWN	Resistor-Weighted Network

Chapter 1

Literature Review

1.1. Operational Amplifiers

1.1.1. Basic Principles

An operational amplifier or "op-amp" is a type of differential amplifier. Fundamentally, these amplifiers multiply the difference between the voltages at their positive (V^+) and negative (V^-) terminals by a specified gain factor. This gain, A_d , is also known as the *differential-mode gain*. Although differential amplifiers are often designed for a specific A_d , op-amps usually aim to have as high a differential gain as possible (for an ideal op-amp, $A_d \rightarrow \infty$).

A_d is also known as the *open-loop gain*. Due to a large-valued open-loop gain, op-amps are often used in *closed-loop* configurations, which are more flexible and take advantage of this large A_d . These configurations arise when there is a negative feedback loop from the output which is connected to the negative input terminal.

1.1.2. Limitations

Often, it is applicable to design an amplifier circuit using the ideal operational amplifier model. This model assumes no current into the input terminals, an infinite, linear, differential-mode gain, and that terminal voltage $V^+ = V^-$ when negative feedback is present. This model, however, may be inadequate in low voltage, high current or high frequency environments. The following are common limitations of non-ideal op-amps [1]:

- Voltage supply saturation. For given k , output cannot go above $V_{ss} - k$ or below $V_{dd} + k$.
- Finite bandwidth. Output signal magnitude reduces at high frequencies. This effect can be analysed using the gain-bandwidth product (GBWP) equation.
- Offset voltage/bias current. Even with no input, there exists a small "offset voltage" and "bias current" into the amplifier. This results in unwanted voltage at the output.
- Finite slew rate. The output cannot change quicker than a specified rate. This is different to the finite bandwidth limitation, but has a similar limiting effect.
- Finite common-mode rejection ratio (CMRR). An op-amp should ideally only amplify $V_+ - V_-$, but also amplifies the unwanted common signal (e.g. noise) on both inputs.

1.1.3. Key Specifications

Based around the above limitations, op-amp datasheets provide a number of key specifications that may be important for design. The op-amp used in this project is the MCP6242. Listed below are its notable specifications [2]:

- Typical CMMR of 75 dB (DC) to 65 dB (1 kHz).
- Ability to output between 0.035 and 5.465 V if $V_{ss} = 5.5$ V and $V_{dd} = 0$ V.
- Slew rate of 0.3 V/uS.
- Common mode input range from $V_{dd} - 0.3$ V to $V_{ss} + 0.3$ V.
- Maximum current output of 23 mA.
- Gain-bandwidth product of 550 kHz.

1.1.4. Configurations

A number of well-known op-amp configurations exist that all achieve slightly different amplification goals. The following list compares some common configurations [3]. Although certain circuits have two inputs, one of the inputs can be set to a specific voltage level for to add an offset to the output. These configurations can also be expanded to allow for signal "summing" by simply adding more inputs in parallel.

Type	Advantages	Disadvantages
Non-inverting	- Simple to design and build - High input impedance	- Large input bias currents - Amplifies noise from input
Differential	- Good noise rejection - Flexible	- Complex design - Low input impedance
Instrumentation	- Same as differential - Very high input impedance	- Complex and expensive design

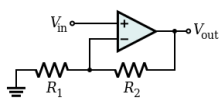


Figure 1.1:
Non-Inverting
Amplifier [5]

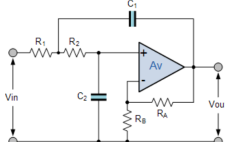


Figure 1.2:
Modified
Non-Inverting
Amplifier [6]

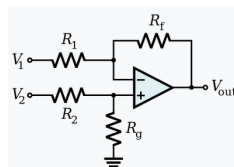


Figure 1.3: Dif-
ferential Ampli-
fier [5]

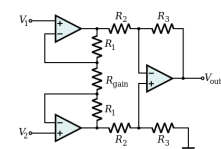


Figure 1.4: In-
strumentation
Amplifier [5]

1.2. Current Sensing

1.2.1. Techniques

Measurement techniques are usually either "invasive" or "non-invasive". Invasive techniques need to be built into the circuit directly and can have a significant affect on its operation, whereas non-invasive techniques may be added after the initial circuit design e.g. by measurement of a conductor's magnetic field. A list of a few of these techniques [7] include:

- A current-sensing resistor in series, which uses Ohm's law with a voltage measurement to calculate current.
- Hall element sensors, which measure the potential difference created as a result of the main current's magnetic field bending another current left/right.
- Direct coil techniques, which make use of Faraday's law.

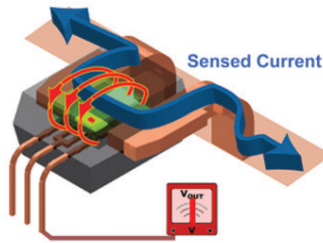


Figure 1.5: Hall Effect Sensor Working Principle [9]

1.2.2. High-Side vs Low-Side

This distinction refers to the placement of a current-sense element (e.g. resistor) relative to the load. For circuits which draw higher currents, high-side sensing can be used (placing the resistor closer to the positive side of the voltage source) and is often more convenient. Low-side sensing, on the other hand, can potentially cause ground loop issues [8], but has the ability to detect faults (e.g. short-circuits) earlier.

1.2.3. AC, DC and Power Requirements

As mentioned, there are various non-invasive and even wireless techniques used to measure current. Coil techniques make use of induction and therefore require AC to operate. The Hall effect and sense resistors, on the other hand, may be used in the DC case. Wireless techniques have benefits over resistors in that they can be configured to draw much less power, whereas sense resistors usually require high power handling capabilities as they pass all current drawn by the actual load through them.

1.3. Ultrasonic Sensors

1.3.1. Interfacing with the Range Sensor

The HC-SR04 ultrasonic ranging module's interface will be discussed. It has 4 pins, namely V_{cc} , GND , $Trig$ (*Trigger*) and $Echo$. It should be powered with $5 V_{dc}$ and requires at least 15 mA to function, meaning it will dissipate 75 mW of power. First, $Trig$ should be pulled high to indicate that the device should send a burst of ultrasonic sound out. Then, if the sound wave is received back, the device will output a distance-proportional pulse on the $Echo$ pin.

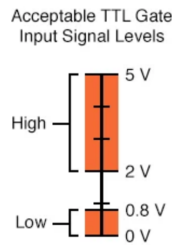


Figure 1.6: TTL Input/Output Levels [10]

The following detailed procedure should be followed to make a distance measurement [3]:

1. A pulse of at least $10 \mu\text{s}$ should be output onto $Trig$. This pulse must be TTL compliant as indicated in Figure 1.6 i.e. between 2 and 5 V.
2. If the sound wave is received back by the sensor, $Echo$ (also TTL) will go high for t_{high} seconds, where t_{high} is the time it took the wave to return to the sensor. This signal should therefore be conditioned if a circuit which requires 3.3 V is used.
3. The distance can then be calculated. One of the following methods may be used:
 - (a) The length of time of the $Echo$ output signal can be digitally measured and the distance then calculated using $Distance = \frac{t_{high} * v_{sound}}{2}$ (1.1) [3].
 - (b) The output pulse can be converted to an analog signal using filtering. The resultant filtered voltage will also be proportional to t_{high} .
4. A minimum of 60 ms should be present in between each pulse. This allows for a theoretical range of $\frac{60 \text{ ms} * 340 \text{ ms}^{-1}}{2} = 10.2 \text{ m}$. In practice, the device has a range of $\approx 4 \text{ m}$.

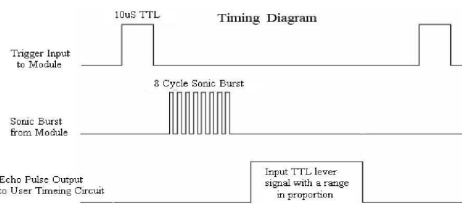


Figure 1.7: Sensor Timing Diagram [3]

1.3.2. Fundamental Operation of Range Sensors

Sound Transducers

Ultrasonic sensors work by emitting and receiving sound waves of a high frequency. Electrical "transducers" are used to convert between electrical/sound energy. These are either excited by an electrical signal and caused to vibrate, or vibrate due to an incoming sound-wave and then generate an electrical signal. The two main transducer types used in ultrasound include [19]:

- *Piezoelectric* transducers. These use a vibrating crystal quartz which deforms in response to a changing potential difference.
- *Capacitive* transducers. These make use of a flexible dielectric membrane attached to an electrode. This electrode is attracted and repelled by electrical charges.

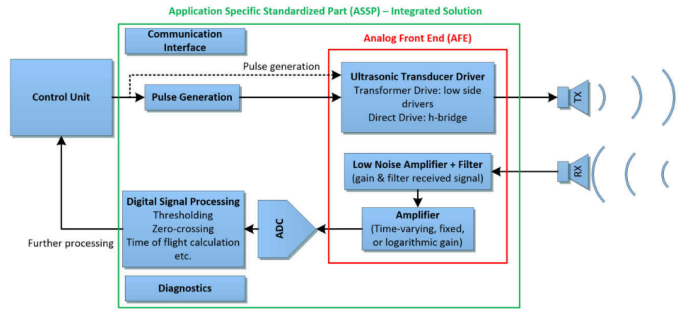


Figure 1.8: Simple Ultrasonic Sensing System [20]

Pulse Generation

Ultrasonic systems generally contain a digital control unit [20]. This unit is responsible for receiving the trigger signal from the communication interface and generating a pulse to send to the Analog Front End (AFE). This pulse is usually sinusoidal and is at a much higher frequency than the trigger input (between 30 kHz and 5 MHz). After the digital pulse is generated, the AFE amplifies it using a transistor drive circuit. This can be at a relatively low voltage e.g. 5 V, but often high-voltage and "direct drive" amplification is used, which may allow up to 36 V.

Pulse Acquisition

After some time, the pulse may return and electrically excite the microphone transducer. It is subsequently filtered and passed through a low-noise amplifier. The signal is then converted by an ADC and enters the digital domain, where further processing is done. Finally, a DSP analyzes the signal. This includes performing the actual "time-of-flight" calculation, which it then communicates back to the control unit. The control unit is then responsible for creating the echo signal on the communication interface for the length of time sent by the DSP.

1.4. PWM to Analog Conversion

PWM (Pulse Width Modulation) is useful in that it allows analog information to be conveyed in digital signals. PWM waves are similar to square waves, however differ in that $t_{high} \neq t_{low}$. A PWM signal is defined by 3 properties:

- Frequency: The rate at which the signal oscillates. $f = \frac{1}{t_{high}+t_{low}}$ Hz.
- Amplitude: The difference between "high" and "low" voltages. $A = V_{high} - V_{low}$ V.
- Duty cycle: The ratio of the signal's "high time" to its period. $\tau = \frac{t_{high}}{t_{high}+t_{low}}$ s.

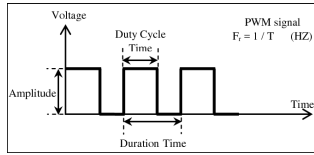


Figure 1.9: PWM Signal Voltage vs Time [11]

Often, this analog information is conveyed in a varying duty cycle (τ). To convert this varying value to analog, a low-pass filter can be used. Since the signal's average value increases with τ , filtering out all "harmonics" of the signal will result in $V_{out} = A \times \tau$ (1.2) [12]. The cutoff frequency (f_c) of the filter should be as low as possible, while maintaining an acceptable rise time, in order to minimize ripple on the filter output. Then, since $t_r \propto \frac{1}{f_c}$, $t_{r(max)}$ will determine the minimum cutoff frequency, $f_{c(min)}$. This will be based on the filter used e.g. $f_{c(min)} = \frac{3.3}{2\pi \cdot t_{r(max)}}$ for a 2nd order filter [C.1.1].

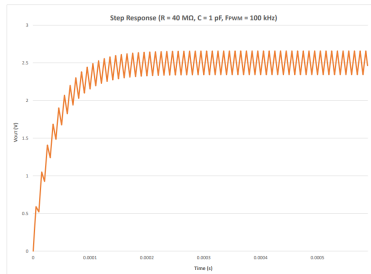


Figure 1.10: Filtered PWM Signal [12]

Assuming $f_{c(min)}$ is fixed, $f_{c(max)}$ should be determined by the maximum acceptable noise on the output of the filter. Since filtering will still leave a small "ripple" signal at frequency f_{PWM} , this will be the largest noise component. Given the following:

- A : Amplitude of the PWM signal (V)
- τ_{max} : Maximum duty cycle of the PWM signal (%)
- N_{max} : Maximum acceptable noise of the filtered output (V)

Then the required attenuation at f_{PWM} is given by $A_{dB} = 20 \log \left[\frac{A \cdot \tau_{max}}{N_{max}} \right]$ (1.3). This will determine $f_{c(max)}$, in conjunction with the type of filter used and its order.

1.5. Digital to Analog Conversion

1.5.1. Configurations

A DAC can be implemented using different summing op-amp configurations:

- *Inverting vs Non-Inverting.* Single-supply inverting amplifiers require an offset bias at V^+ to keep the output positive. Non-inverting amplifiers suffer from input source coupling (discussed in Section 1.5.2) and require a second stage to invert the output.
- *Resistor-Weighted vs R2R Ladder.* Resistor-weighted networks (RWN) use resistors continuously halving in value (e.g. in Figure 1.11). They are simple to build, but require large-valued precision resistors, or many parallel resistors. R2R Ladder networks (e.g. in Figure 1.12) solve this by re-using resistors across inputs.

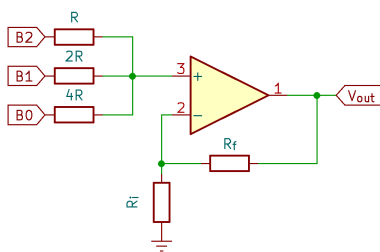


Figure 1.11: Non-Inverting Mode with Resistor-Weighted Network [22]

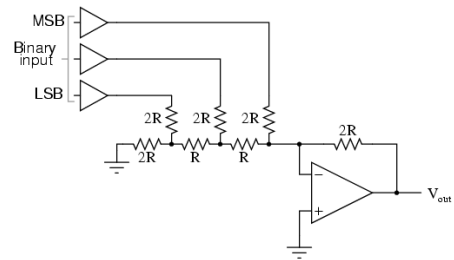


Figure 1.12: Inverting Mode with R2R Ladder Network [23]

Common-mode voltage range limitations should be considered. In inverting mode, V^- is a "virtual ground" due to negative feedback. This means common-mode voltage always equals the offset voltage at V^+ . Rail voltage can therefore be chosen using only this voltage and the output specifications. This is not true in non-inverting mode: the voltage at V^+ changes based on the source voltages. For a DAC using the MCP6242, this means $V_{dd} \geq V_{digital} - 0.3V$.

1.5.2. Impedance Requirements

For a practical source, $R_o \neq 0\Omega$, meaning amplifier input impedance should be considered. Non-inverting amplifiers do not have a "virtual ground", meaning sources are not decoupled from each other [22] causing some noise. Table 1.1 documents lowest input impedances:

Configuration	R2R	RWN
Inverting	$2R$	R
Non-Inverting	$4R$	$R \times \left(1 + \frac{1}{\frac{1}{2} + \frac{1}{4} + \dots + \frac{1}{2^N}}\right) \approx 2R$

Table 1.1: Input Impedance of Various Summing Configurations

For a practical load, $R_L \neq \infty$, meaning amplifier output impedance should be considered. A buffer stage can be added. This lowers the output impedance of the op-amp.

1.6. Lead-Acid Batteries

Lead-acid battery cells permit a range of charging voltages. The voltage values are dependent on a number of factors, namely how the battery will be used, the ambient temperature, the stage in the charging cycle, and, of course, the number of cells.

If the battery is to be used regularly, it is said to be in "cycle" mode and should be charged at the "cycle" voltage. "Standby" or "floating" voltage levels are also possible for prolonged life and less regular use-cases. The ambient temperature also influences the desired voltage, with hotter temperatures requiring lower charge voltages.

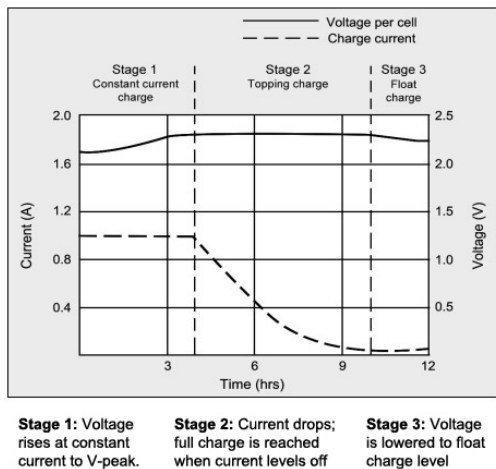


Figure 1.13: The 3 Charging Stages for Lead-Acid Batteries

These batteries should be charged in a three-stage process [30], as seen in Figure 1.13. For stage 1 and 2, the cycle voltage is applied until the current reduces to a small value. In stage 3, the slightly lower "float" voltage should then be applied. This helps keep the battery at a high enough voltage to prevent damage due to self-discharge.

Charging voltages are typically specified "per-cell". A typical cycle voltage is between 2.40 and 2.45 V · cell⁻¹, while a typical float voltage is between 2.30 and 2.35 V · cell⁻¹ [30]. Charging currents may be chosen based on lifetime requirements, however most manufacturers recommend a limit of 0.3 C or 0.3 times the rated capacity of the battery. Slightly higher currents may be allowed while the cells are still at low capacity, and slightly lower currents may be used to prolong the life of the battery. During float-charging, the battery typically draws around 0.001C [31].

The RT670 supplied for this project has 3 cells and can charge at a cycle voltage of between 7.30 to 7.40 V i.e. around 2.45 V · cell⁻¹ [32]. Its technical maximum charging current is 2.10 A and, since its capacity is 7 Ah, this indicates a charge rating of 0.3 C as expected. The RT640, also supplied for this project, has similar specifications, except permits a charging current of 1.2 A and a slightly wider cycle voltage range.

Chapter 2

Detailed Design

2.1. System Design

The final block diagram for the system can be found in Figure 2.1.

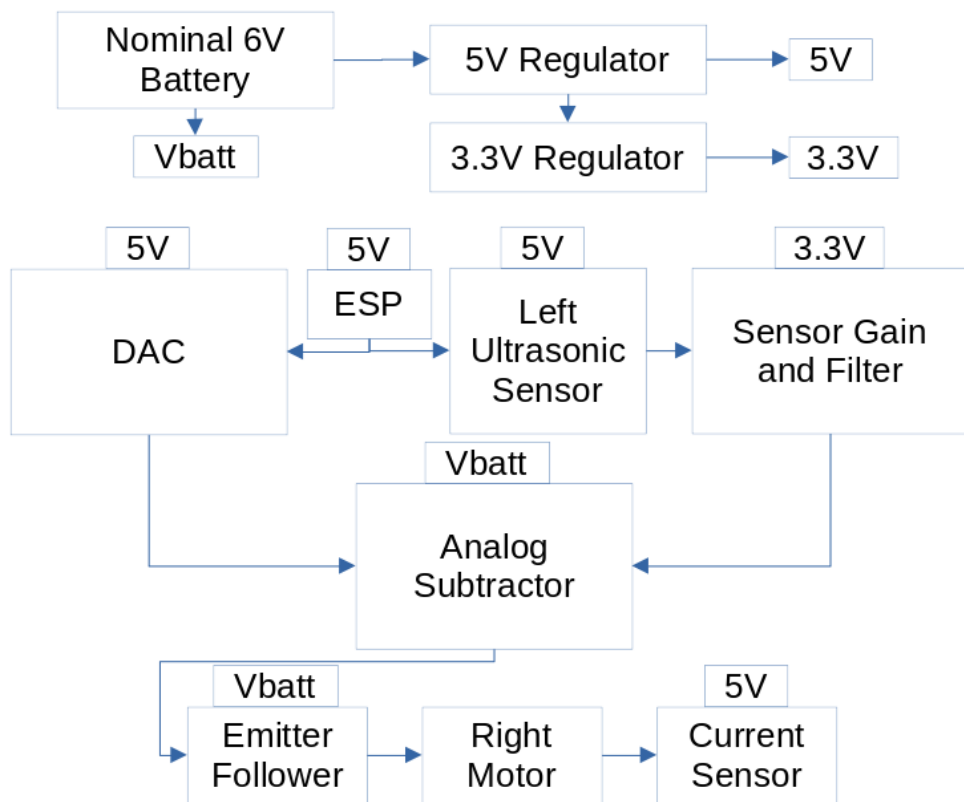


Figure 2.1: Final System Block Diagram

2.2. Voltage Regulation

The LD1117V and LD33CV will be used for 5 V and 3.3 V regulation respectively. The circuit diagram for both circuits is shown in the figures below. The LD33CV has a maximum dropout voltage of 1.3 V [27]. This means that it can safely be powered directly from the 5 V regulator, as $5\text{ V} - 1.3\text{ V} = 3.7\text{ V}$. The variable LD1117V also has a maximum dropout voltage of 1.3 V [27], and can handle an input operating voltage of maximum 15 V. This means it can safely be powered from the maximum 7.2 V battery supply, however will suffer when the supply drops below 6.3 V. Under-voltage protection should therefore be implemented.

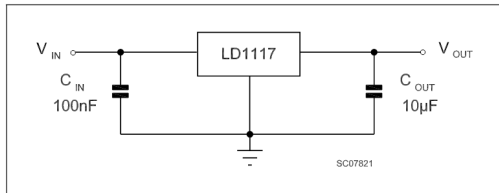


Figure 2.2: 3.3 V Circuit [27]

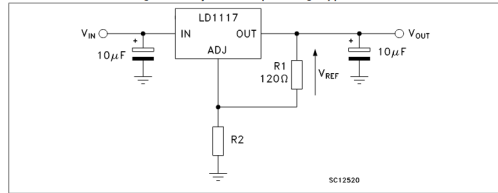


Figure 2.3: 5 V Circuit [27]

The feedback resistor values simply need to be calculated. According to [27], R_2 in Figure 2.3 can be calculated using $V_{out} = V_{ref}(1 + \frac{R_2}{R_1})$. With $V_{out} = 5\text{ V}$, $V_{ref} \approx 1.25\text{ V}$, and $R_1 = 120\Omega$, $R_2 = R_1 \cdot \left(\frac{V_{out}}{V_{ref}} - 1\right) = 360\Omega$. A 470Ω potentiometer will be used for the practical circuit to adjust the output to exactly 5 V.

2.3. Current Sensor

2.3.1. Configuration

The non-inverting amplifier configuration will be used for the current sensor. The gain, noise and rise time requirements should be analyzed to determine whether a first or second order filter should be used.

2.3.2. Gain

The gain of the amplifier should be determined such that, when the maximum current flows through the sense resistor, the maximum voltage is output. The maximum current of the motor should therefore be measured. This can be done by connecting the motor to a power supply (through an ammeter), stalling the motor, and reading the output current.

With a supply voltage of 6.4 V connected, the motor for this project read 740 mA, however different configurations may read between 1 and 1.5 A depending on the supply voltage and motor. The average free-running current, however, is around 200 mA, and therefore a value of $I_{max} = 400$ mA will therefore be chosen to allow for some headroom while still maintaining adequate resolution.

Since a sense resistor of $10\text{ m}\Omega$ is to be used, the maximum voltage through this resistor will therefore be 4 mV. Although this voltage level is small, it is expected, given that the resistance value is so small. It is also desirable, as it shows that the circuit is not "stealing" too much power from the motor itself. Since it is not required to measure the motor current when stalled, gain will be calculated based on a 5 V maximum rail voltage. A gain of $\frac{3.3\text{ V}}{4\text{ mV}} = 825$ is therefore chosen.

2.3.3. Filter

The requirements specify that a 10 mV signal at 1 kHz should be attenuated to less than 250 mV, i.e. should only have a gain of 25 and not 500. This means that that a 1 kHz signal should be attenuated by $20 \log(\frac{825}{25}) \approx 30$ dB. The specifications also require that the rise time, $t_r < 100$ ms. For a first order filter, this attenuation occurs at $10 \log \left[1 + \left(\frac{1\text{ kHz}}{f_{c(max)}} \right)^2 \right] = 26 \therefore f_{c(max)} = 32\text{ Hz}$ [C.1.1]. Also, the minimum frequency that will satisfy the rise time requirements for a first order filter is calculated using $f_{c(min)} = \frac{2.2}{2\pi t_r} = 3.5\text{ Hz}$ [C.1.1]. This shows that a first-order filter is adequate. A cutoff of $f_c = 10\text{ Hz}$ is therefore chosen as a compromise between the two specifications.

2.3.4. Design

Since a 1st order filter will be used, a simple resistor-capacitor combination will be placed before the positive terminal. Also, high resistor values should be chosen to limit current to below 150 uA.

- Assuming $i_n = 0$, choose $\frac{V_{out(max)}}{R_1+R_f} << 150\mu A \therefore R_1 + R_f >> 33\text{ k}\Omega$. Choose $R_f = 100\text{ k}\Omega$.
- Since gain $G = 1 + \frac{R_f}{R_1} = 825$, $R_1 \approx 120\Omega$.
- Choose $C_i = 100\text{ nF} \therefore R_i = \frac{1}{2\pi \cdot 10\text{ Hz} \cdot 100\text{ nF}} = 160\text{ k}\Omega$. Choose $R_i = 150\text{ k}\Omega$ for $f_c \approx 11\text{ Hz}$.

2.3.5. Circuit Diagram

The following figure details the final circuit design for the sensor and amplifier system.

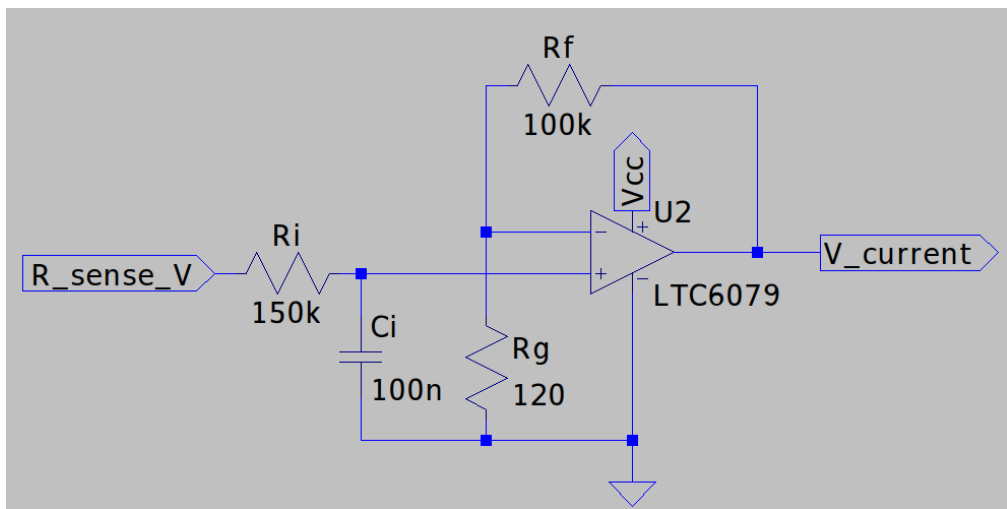


Figure 2.4: Current Sensor Circuit Diagram

A 3.3 V supply will be used to limit the voltage into the ESP, which will be reading the current sensor output. Although there are benefits to a dual rail supply, that would prove impractical in the context of the larger system.

2.4. Ultrasonic Sensor

2.4.1. Power and Output Requirements

The range sensor requires 5 V_{dc} power and will draw around 15 mA. Since the LD1117V provides a stable 5.0 V output and is capable of providing up to 800 mA of current, the sensor will be powered directly from this regulator.

The sensor's echo output is a PWM wave of varying duty cycle τ and $f_{PWM} = 16$ Hz. This signal's amplitude could be as high as 5 V (TTL level). The maximum output A_{max} after unity filtering, however, will be determined by the maximum duty cycle, t_{max} . Since a distance of $D_{max} = 1$ m and $D_{min} = 5$ cm, Equations 1.1 and 1.2 can be used to calculate:

- At D_{max} , $t_{max} \approx 5.9$ ms, $\tau_{max} = \frac{5.9\text{ ms}}{1/16} \approx 9.5\%$ and $A_{max} = (5\text{ V}) \cdot (9.5\%) = 475$ mV.
- At D_{min} , $t_{min} \approx 0.29$ ms, $\tau_{min} = \frac{0.29\text{ ms}}{1/16} \approx 0.47\%$ and $A_{min} = (5\text{ V}) \cdot (0.47\%) = 23$ mV.

2.4.2. Filter Selection

To determine the filter's order, rise time and noise requirements should be considered:

- After filtering, since gain $\approx \frac{3\text{ V}}{475\text{ mV}} \approx 7\text{ V/V}$, filter ripple must be under $\frac{70\text{ mV}}{7} = 7$ mV.
- A 10% to 90% rise time (t_r) of 1.5 s should be adhered to.

These specifications result in the requirement that A_{dB} at $f_{PWM} = 20 \log \left[\frac{5\text{ V}}{7\text{ mV}} \right] \approx 60$ dB. A 3rd order filter with $f_c = 1$ Hz will be used, as a 2nd order may be tolerance-sensitive. This provides $t_r \approx 0.63$ s and $A_{dB} \approx 72$ dB [C.1.1].

Filter type	Design Spec.	Cutoff f_c	Rise time t_r	Attenuation A_{dB}
1 st order	Rise Time	0.233 Hz	1.5 s	37 dB
	Attenuation	0.016 Hz	22 s	60 dB
2 nd order	Rise Time	0.350 Hz	1.5 s	66 dB
	Attenuation	0.505 Hz	1.038 s	60 dB
3 rd order (cascade)	Rise Time	0.420 Hz	1.5 s	95 dB
	Attenuation	1.600 Hz	0.394 s	60 dB

Table 2.1: Filter type vs Rise Time and Attenuation using [C.1.1]

2.4.3. Configuration

A "two-and-a-half" stage configuration will be used. The first stage is a gain/offset and 1st order filter, and is placed first in order to amplify the signal above the MCP's 35 mV floor. The second stage is unity-gain 2nd order filter. A non-inverting amplifier will be used for stage 1, and a Sallen-Key topology for stage 2. Since the quiescent current for each op-amp is 70 μA [2], stage 1 & 2 will be allocated 400 μA and 200 μA respectively.

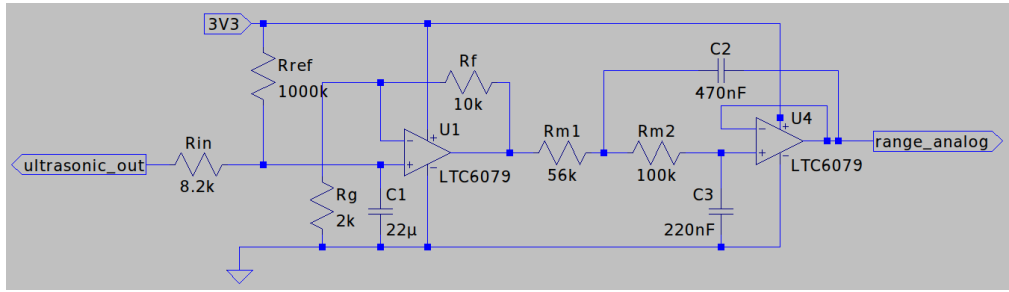


Figure 2.5: Range Sensor Amplifier Circuit Diagram

2.4.4. Gain Stage

This stage will be powered by the 3.3 V regulator. As this is a low-gain circuit, input bias voltages can be neglected. Slew rate and CMMR imbalance can also be ignored due to the low-frequency, single-ended use of the op-amp. Voltage rail saturation does not need to be considered at the circuit output, as $0.3 \text{ V} < V_{out} < 3 \text{ V}$, and has already been catered for at the input, as discussed in Section 2.4.3. Using the equations at [18], and the expected input ranges from the filter stage, gain $m = \frac{3\text{V}-0.3\text{V}}{475\text{mV}-23\text{mV}} = 5.97 \text{ V V}^{-1}$, and offset $b = 0.3 \text{ V} - m \times 23 \text{ mV} \approx 163 \text{ mV}$:

- With idle current $I_Q = \frac{V_{out}}{R_f + R_g}$, and $V_{out(max)} = 3.3 \text{ V}$, $(R_f + R_g)_{min} = \frac{3.3 \text{ V}}{400 \mu\text{A}} = 8.25 \text{ k}\Omega$.
- Since the offset voltage is low, R_{ref} will be high. A potentiometer will also be used to tune this offset, therefore choose $R_{ref} = 1000 \text{ k}\Omega = 820 \text{ k}\Omega + 470 \text{ k}\Omega\text{pot}$.
- Calculate $R_{in} = \frac{R_{ref} \times b}{V_{ref} \times m} \approx 8.2 \text{ k}\Omega$ with $V_{ref} = 5 \text{ V}$ and $C_1 = \frac{1}{2\pi f_c R_1} \approx 22 \mu\text{F}$.
- Choose $R_f = 10 \text{ k}\Omega$ to satisfy the current requirements.
- Calculate $R_g = \frac{R_{ref} \times R_f}{m \times (R_{in} + R_{ref}) - R_{ref}} \approx 2 \text{ k}\Omega$. To tune the gain, choose $R_g = 1.5 \text{ k} + 1 \text{ k}\Omega\text{pot}$.

2.4.5. Filter Stage

This stage will use the 3.3 V regulator to clip the circuit output for use with the MCU. This results in the 2nd order stage transfer function $H(s) = \frac{1}{1+0.2251s+0.02533s^2} = \frac{1}{1+a_1s+b_1s^2}$ with $\zeta = 0.707$. Now, component values can be chosen. Formulae from [17] will be used:

- Since both capacitors are open-circuit during DC, the idle current is very low. A maximum step input will result in a surge of current through C_2 to ground. With $V_{in(max)} = 5 \text{ V}$, $(R_{m1} + R_{m2})_{min} = \frac{5 \text{ V}}{200 \mu\text{A}} = 25 \text{ k}\Omega$.
- Since $C_3 = \frac{a_1}{2\pi f_c(R_{m1} + R_{m2})}$ [17], choose $C_3 = 220 \text{ nF}$ so that $R_{m1} + R_{m2} \approx 160 \text{ k}\Omega$.
- To meet $C_2 \geq C_3 \cdot \frac{4 \cdot b_1}{a_1^2} \approx 2C_3$ [17], choose $C_2 = 470 \text{ nF}$.
- Since $C_3 \cdot C_2 = \frac{b_1}{((2\pi f_c)^2 R_{m1} R_{m2})}$, and $R_{m1} + R_{m2} = 450 \text{ k}\Omega$, solve to obtain $R_{m1} = 61 \text{ k}\Omega$ and $R_{m2} = 99 \text{ k}\Omega$. Choose $R_{m1} = 56 \text{ k}\Omega$ and $R_{m2} = 100 \text{ k}\Omega$ as practical values.

2.5. Digital to Analog Converter

2.5.1. Configuration and Impedance Requirements

The inverting, R2R configuration will be used. A voltage divider will be added at V^+ to offset the negative gain, and a buffer stage will be used for better output current. The ESP32 pin output impedance is typically $30 - 40 \Omega$ [24]. In order to have less than 1% deviation of this source voltage, R_{in} can be solved for using:

$$\frac{V_{cc} - V_{pin}}{V_{cc}} = \frac{R_{in}}{R_{in} + R_{ESP}} \leq 0.01 \therefore R_{in} \geq 3.5 \text{ k}\Omega$$

The output impedance of the MCP is $R_o \approx \frac{5.5 \text{ V}}{23 \text{ mA}} = 239 \Omega$ [2]. The MCP also has current protection, and can continuously source/sink 23 mA to a 0 ohm load. A buffer stage will decouple the negative feedback loop of the summer from the load stage, adding protection.

2.5.2. Summing Stage

All ESP pins are either 0 or 3.3 V. An amplifier current limit of $250 \mu\text{A}$ (after quiescent current), and a pin limit of $50 \mu\text{A}$ per digital input is chosen. Since an inverting configuration with a virtual ground (which will be $<< 3.6 \text{ V}$) has been used, the common-mode range of the op-amp is not violated. Since the MCP can only reach within 35 mV of the rails, an output range of $0.1 \text{ V} < V_{out} < 3.1 \text{ V}$ will be designed for. Both stages can be powered by 5 V.

- For amplifier current, $R_f > \frac{3.3 \text{ V}}{250 \mu\text{A}} = 13.2 \text{ k}\Omega$. For input current, $2R > \frac{3.3 \text{ V}}{50 \mu\text{A}} = 66 \text{ k}\Omega$.
- Choose $2R = 100 \text{ k}\Omega$. For 1111, and using the summing amplifier formula (before offset), $V_{out} = -3 \text{ V} = - \left[\frac{R_f}{2R} \times 3.3 + \frac{R_f}{4R} \times 3.3 + \frac{R_f}{8R} \times 3.3 + \frac{R_f}{16R} \times 3.3 \right] \therefore R_f = 48.485 \text{ k}\Omega$. A potentiometer will be used to tune the gain, therefore choose $R_f = 47 \text{ k}\Omega + 4.7 \text{ k}\Omega\text{pot}$.
- For $V_{out} = 3.1 \text{ V}$ with 0000 input, $V^+ = V^- = 3.1 \text{ V} \times \frac{50 \text{ k}\Omega}{48.485 \text{ k}\Omega + 50 \text{ k}\Omega} \approx 1.574 \text{ V}$. For the voltage divider, choose $R_a = 47 \text{ k}\Omega \therefore R_b = 21.59 \text{ k}\Omega$. A potentiometer will be used to adjust the offset voltage, therefore choose $R_b = 18 \text{ k}\Omega + 10 \text{ k}\Omega\text{pot}$.

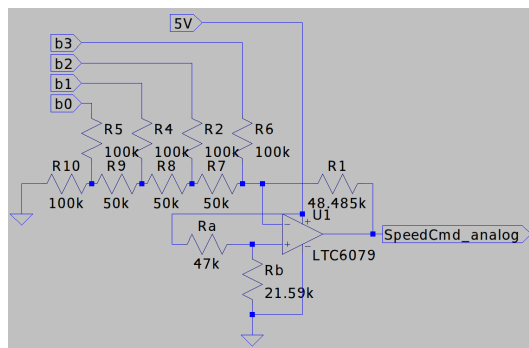


Figure 2.6: Digital to Analog Converter Circuit Diagram

2.6. Analog Motor Controller

2.6.1. Configuration

The analog motor controller circuit will consist of both a subtractor stage and a power stage. The subtractor will be a differential op-amp which will receive the range sensor and DAC outputs as inputs. The output of this stage will feed the power stage with the "motor control" command. The power stage will use a common-collector circuit with a TIP31C NPN transistor to provide current gain from the control command. A second transistor, the 2N2222A, will be used to create a Darlington pair configuration to increase the input impedance. A "flyback" diode will be connected from ground to the power stage's output to prevent sparking.

2.6.2. Power Stage

Since the load is a motor, current will always be sourced by the transistor (not sunk), and therefore the load can be connected directly to the emitter without any bias resistor or AC coupling capacitor. Since the subtractor stage can provide a DC bias, there is also no need for a resistor input bias network.

According to the specifications, the output voltage range across the motor/load should ideally be $0.5 \text{ V} < V_L < 6.2 \text{ V}$, however leniency has been provided due to op-amp current capabilities. The TIP31C saturates at $V_{be} \approx 0.7 \text{ V}$ for $I_c = 10 \text{ mA}$ and at $V_{be} \approx 0.95 \text{ V}$ for $I_c = 1 \text{ A}$ (around the motor stall current) [4], and the 2N2222A has $V_{be(on)} \approx 0.6 \text{ V}$ [26]. Therefore, to ensure the motor is off, $V_{control} < 0.5 + 0.7 + 0.6 = 1.8 \text{ V}$, and to power the motor fully, $V_{control} > 6.2 + 0.95 + 0.6 = 7.75 \text{ V}$. A range of $1.8 \text{ V} < V_{control} < 7.2 \text{ V}$ is therefore chosen. With $I_{c(max)} \approx 1 \text{ A}$, the source needs to be capable of providing $I_{s(max)} = \frac{1 \text{ A}}{\beta_1 \beta_2} < 1 \text{ mA}$ since $\beta_1 \approx 10^{1.4} = 25$ [4] and $\beta_2 \approx 150$ [26].

2.6.3. Subtractor Stage

The input voltage ranges into this stage are $0.2 \text{ V} < V_{range} < 3.3 \text{ V}$ for the ultrasonic sensor, and $0.1 \text{ V} < V_{speed} < 3.1 \text{ V}$ for the DAC. Since the car chassis has a maximum width of around 15 cm, the minimum "stop" value for V_{range} will be chosen to be 20 cm to allow for a full turn when approaching an object. This corresponds to $V_{range(min)} \approx 0.6 \text{ V}$.

Since a high V_{speed} corresponds to a low output voltage, the DAC input will be connected to the inverting terminal. No offset needs to be added at the non-inverting terminal as the range sensor provides a constant 3.3 V when no object is near. A limit of $400 \mu\text{A}$ should be kept for this circuit, excluding quiescent current. Referring to the final circuit diagram in Figure 2.7 below and according to [25], the equation for $V_{control}$ is given by:

$$V_{control} = \left(V_{range} \cdot \frac{R_a}{R_a + R_b} \right) \left(1 + \frac{R_f}{R_s} \right) - V_{speed} \cdot \frac{R_f}{R_s} \quad (2.1)$$

It should be noted that, given the specifications, there are 4 conditions that should be met:

Condition	V_{speed}	V_{range}	$V_{control}$
1	0.1 V	0.6 V	< 1.8 V
2	0.1 V	3.3 V	> 7.2 V
3	3.1 V	0.6 V	< 1.8 V
4	3.1 V	3.3 V	< 1.8 V

Table 2.2: Output Conditions for Various Range and Sensor Inputs

Condition 3, however, will always be true, given that condition 1 is true (due to the nature of the subtractor). Component values can now be calculated:

- Maximum current will flow through the feedback loop when $V_{control} = 7.2 \text{ V}$ and $V_{speed} = 0 \text{ V}$, with a value of $I_{max} = \frac{7.2 \text{ V}}{R_s + R_f}$. To keep feedback current < 200 μA , $(R_s + R_f)_{min} = \frac{7.2 \text{ V}}{200 \mu\text{A}} = 36 \text{ k}\Omega$.
- Conditions 2 and 4 result in a minimum gain of $\frac{7.2 \text{ V} - 1.8 \text{ V}}{3.1 \text{ V} - 0.1 \text{ V}} = 1.8 \text{ V/V}$. Choose a gain of 2 i.e. $\frac{R_f}{R_s} = 2$. Choose $R_f = 47 \text{ k}\Omega$ and $R_s = 23.5 \text{ k}\Omega$. A potentiometer will be used for fine-tuning of the speed gain $\therefore R_s = 18 \text{ k}\Omega + 10 \text{ k}\Omega\text{pot}$. It can now be found that $V_{control} = 3 \cdot V_{range} \cdot \frac{R_a}{R_a + R_b} - 2 \cdot V_{speed}$.
- Applying condition 1, $1.8 \text{ V} > 3 \cdot 0.6 \text{ V} \cdot \frac{R_a}{R_a + R_b} - 2 \cdot 0.1 \text{ V} \therefore \frac{R_a}{R_a + R_b} < 1.111$.
- Applying condition 2, $7.2 \text{ V} < 3 \cdot 3.3 \text{ V} \cdot \frac{R_a}{R_a + R_b} - 2 \cdot 0.1 \text{ V} \therefore \frac{R_a}{R_a + R_b} > 0.747$.
- Applying condition 4, $1.8 \text{ V} > 3 \cdot 3.3 \text{ V} \cdot \frac{R_a}{R_a + R_b} - 2 \cdot 3.1 \text{ V} \therefore \frac{R_a}{R_a + R_b} < 0.808$.
- Choose $\frac{R_a}{R_a + R_b} = 0.78$. To keep maximum range sensor input current $I_{max} = \frac{3.3 \text{ V}}{R_a + R_b}$ below 200 μA , $R_a + R_b > 16.5 \text{ k}\Omega$. Choose $R_a = 56 \text{ k}\Omega \therefore R_b = 15.79 \text{ k}\Omega$. A potentiometer will be used for fine-tuning of the range gain $\therefore R_b = 10 \text{ k}\Omega + 10 \text{ k}\Omega\text{pot}$.

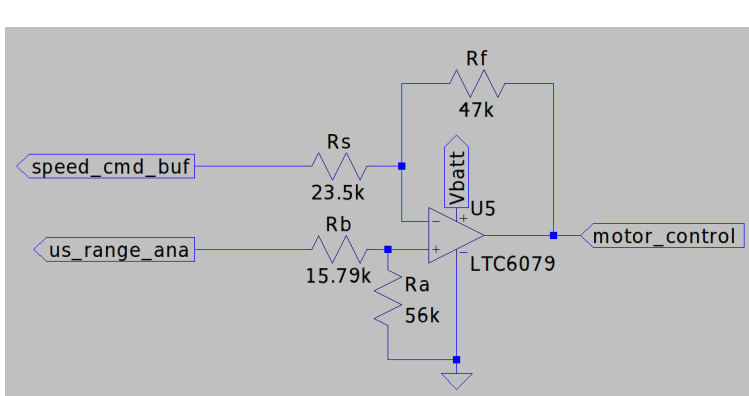


Figure 2.7: Motor Controller Subtractor Stage Circuit Diagram

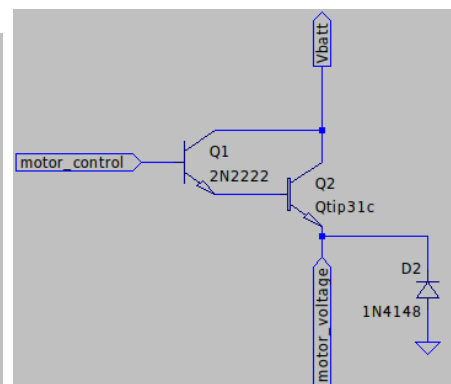


Figure 2.8: Motor Controller Power Stage Circuit Diagram

2.7. Digital Motor Controller: Firmware

2.7.1. Flow Diagrams

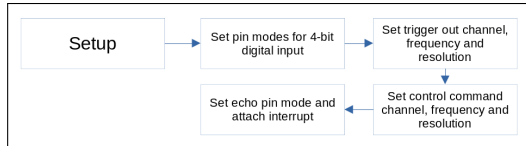


Figure 2.9: Setup Diagram

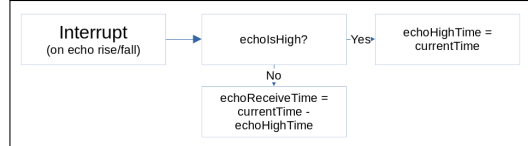


Figure 2.10: Echo Interrupt Diagram

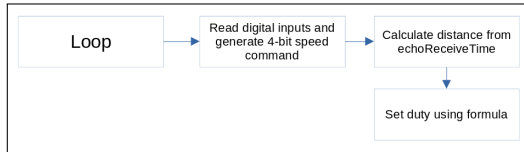


Figure 2.11: Loop Diagram

2.7.2. Range Measurement

As visible in Figure 2.10, range will be calculated by measuring the time that the echo pin is high. An interrupt will be used to detect when the echo output changes from low to high, and vice versa. Then, this time will be divided by two and multiplied by the speed of sound to determine the range of the object. Since the time distance will be in microseconds, the following formula may be used: $D = \frac{t_{us}}{2} \times 343 \text{ m} \cdot \text{s}^{-1} \times 10^{-6}$.

2.7.3. PWM Control

Frequency

If f_{PWM} is too low, the motor switching will be noticeable. If it is too high, the MOSFET will not turn on fast enough. The motor's resistance was measured as $R = 5.3 \Omega$, and inductance was calculated as $L = 1.6 \text{ mH}$ using a frequency test. The motor's cutoff frequency is therefore $f_c = \frac{R}{2\pi L} = \frac{5.3}{2\pi \times 1.6 \times 10^{-3}} \approx 500 \text{ Hz}$. Since the FQD13N06L has a rise time of $t_{r(max)} = 190 \text{ ns}$, signals will only be affected at frequencies near $f_r = \frac{1}{190 \text{ ns}} \approx 5 \text{ GHz}$. $f_{PWM} = 10 \text{ kHz}$ could safely be chosen to ensure adequate filtering of wave harmonics, while not affecting switching times, however $f_{PWM} = 20 \text{ kHz}$ is used to keep the switching frequency above human hearing.

Formula

The digital formula used should emulate the analog motor controller as closely as possible. The controller's range will therefore also be from 20 cm to 1 m and will saturate at "digital rails". Given S , the 4-bit speed command, and R , the range, the following formulae may be used: $C = \bar{R} - (1 - \bar{S})$ with $\bar{R} = \frac{R - R_{min}}{R_{max} - R_{min}}$ and $\bar{S} = \frac{S}{15}$. Finally $duty = clamp(0, C, 1) \times controlResolution$. LEDC functions can then be used [29] to set this PWM appropriately.

2.8. Digital Motor Controller: Switch and Current Sensor

2.8.1. Configuration

The low-side switch will be a FQD13N06L NMOS transistor driven by the ESP using PWM. This transistor was chosen due to its low turn-on voltage, eliminating the need for any gain circuitry. A resistor will be used in series from the ESP to the MOSFET to prevent surge currents due to the capacitive nature of the MOSFET gate. A pull-down resistor will also be used to ensure the circuit is fully off when the ESP pin is in a high impedance state (e.g. when the circuit is powered down or during startup).

The current sensor circuit will also be a non-inverting amplifier with a filter, similar to the circuit used for the analog wheel, however care needs to be taken to ensure the PWM signal is filtered adequately. The sense resistor will be placed on the low side of the MOSFET to avoid the use of a differential amplifier.

2.8.2. Input Resistors

In order to calculate R_a , the series input resistor from the ESP, the assumption is made that the series resistance before the equivalent gate capacitance is zero. Since the current equation for an RC circuit is $I(t) = I_0 e^{-t/\tau}$, with $I_0 = \frac{V}{R}$, the surge current will be I_0 at $t = 0$. Choose $I_0 = 10 \text{ mA}$ $\therefore R_a = \frac{V_{cc}}{I_0} = \frac{3.3 \text{ V}}{10 \text{ mA}} = 330 \Omega$.

The pull-down resistor should be chosen so that the ESP is not loaded during operation, thereby affecting the voltage. If it is chosen that this resistor consumes maximum additional current of $100 \mu\text{A}$, the resistor should then be $R_b(\min) = \frac{3.3 \text{ V}}{100 \mu\text{A}} = 33 \text{ k}\Omega$. Choose $R_b = 100 \text{ k}\Omega$.

2.8.3. Transistor Requirements

It should be checked that the FQD13N06L transistor is suitable with regards to turn-on voltage, current capabilities, and series resistance.

- The V_{gs} threshold voltage should be checked to ensure the transistor is turned on fully. According to [28], the maximum turn-on voltage of the transistor is 2.5 V. Since the ESP will output a 3.3 V PWM signal on its digital pins, the transistor will be turned on fully since the pin's output voltage is 32% higher than the required V_{gs} threshold.
- The current requirements should be compared with the transistor's current capabilities. A maximum stall current of 750 mA is required. If the transistor is not capable of handling this, it might be damaged due to excess heat dissipation. Choose $I_{max} = 1 \text{ A}$ for additional headroom. Again, according to [28], the transistor can handle a continuous current of 7 A with its case kept at 100 °C. This is well within the current limitation of the motor.

- The equivalent series resistance of the transistor should be analyzed at different forward currents in order to determine the voltage drop it will cause in series with the motor. The datasheet reveals that, at $V_{gs} = 5$ V, the forward resistance only varies from around $110\text{ m}\Omega$ to $120\text{ m}\Omega$ as current increases to 10 A. At currents of around 1 A, a maximum voltage drop of around 0.12 V will be found, which is negligible and means that the motor will receive almost the full 7.2 V. This is also at maximum current - at lower current levels, the voltage drop will be even less, however in this design this will be slightly countered by the fact that $V_{gs} = 3.3$ V.

2.8.4. Current Sensor

The same design as in 2.3 will be used. Since a PWM frequency of 20 kHz will be used, the current sensor filtering frequency, which is designed to adequately filter out a 1 kHz signal, is more than adequate, and will filter out the fundamental frequency and all harmonics. The frequency could even be raised, however will be kept the same in order to match it with the analog wheel current sensor.

The rest of the design of the sensor can also be kept identical due to the final receiver of the value (the ESP) being the same. These design decisions, as well as the justifications to keep them, are documented below:

- The non-inverting gain will be 825, which allows for current values of up to 400 mA to be read.
- The filter cutoff frequency will remain at 11 Hz to have a slower response which heavily filters out any noise.
- A 3.3 V supply will be used to limit the output and prevent damaging the ESP's input pins.

2.8.5. Circuit Diagram

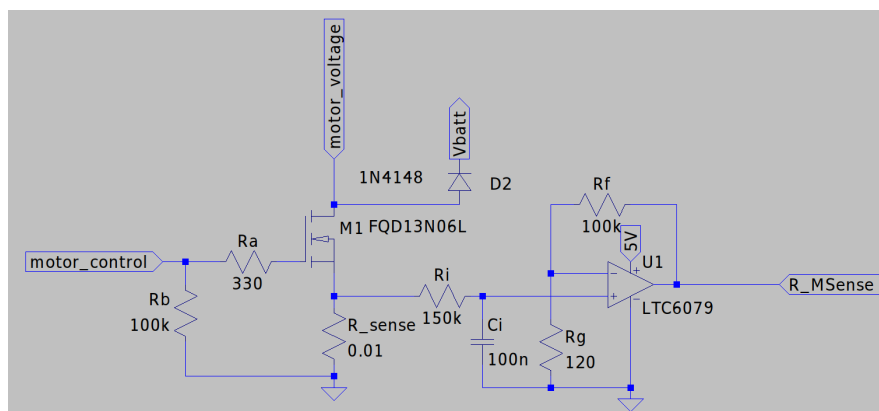


Figure 2.12: Digital Motor Controller and Current Sensor Circuit Diagram

2.9. Battery Charger

2.9.1. Configuration

The supplied battery charger circuit and PCB will be used, with the need to find the relevant resistor values. The circuit has a diode-protected voltage regulator near the input to regulate the 12 V supply down. Then, a current-limiting resistor is used to limit the charging current to the battery. Finally, a low-side NMOS control switch is used to control a high-side PMOS current switch, which charges the battery through a diode.

2.9.2. Voltage and Current Considerations

The battery's voltage and current requirements need to be considered. For cycle use, the battery should be charged at between 7.30 and 7.40 volts, with a maximum current of 2.10 A. For this project, however, it is specified that the circuit should only charge at 0.1C relative to a 4 Ah battery, and therefore a current limit of 400 mA should be adhered to. Lastly, once the cycle voltage has been reached, a maximum of 0.001C current should be allowed into the battery to prevent overcharge, which equates to 4 mA.

2.9.3. Design

Resistor values in Figure 2.13 should now be chosen, as well as transistor components. The IRF9Z24 P-channel MOSFET will be used for M1 due to its continuous current capability of 8.5 A and its low $R_{DS(on,max)}$ of 175 mΩ causing a negligible (4 mV) voltage drop [33]. The 1N5819 diode will be used for both D1 and D2 due to its low turn-on voltage and its high current capabilities. The 2N7000 NMOS transistors will be used for M2, which has no specific requirements. Resistor values may now be calculated:

- The output impedance seen by the battery is $R_o = R_1 \times (1 + \frac{R_4}{R_2})$ [35]. The regulator can be modeled as a voltage source V_{reg} with resistance $R_o = \frac{V_{reg} - V_{diode} - V_{bat}}{I_{bat}}$. To cater for the maximum floating current, condition $R_o > \frac{V_{reg} - V_{diode} - V_{bat(full)}}{4 \text{ mA}}$ must be met, and to cater for a high initial current up to 400 mA, $R_o > \frac{V_{reg} - V_{diode} - V_{bat(empty)}}{400 \text{ mA}}$.
- Choose $V_{bat(full)} = 7.4 \text{ V}$, $\therefore I_{bat} \leq 4 \text{ mA}$ and $V_{diode} \approx 0.15 \text{ V}$ [35]. Choose $V_{bat(empty)} = 6.0 \text{ V}$, $\therefore I_{bat} \leq 400 \text{ mA}$ and $V_{diode} \approx 0.35 \text{ V}$. Using the above, $\frac{V_{reg} - 7.55 \text{ V}}{4 \text{ mA}} < R_o$ and $\frac{V_{reg} - 6.35 \text{ V}}{400 \text{ mA}} < R_o$. Using graphing software, one solution is $R_o = 3 \Omega$ with $V_{reg} \leq 7.56 \text{ V}$ yielding $I_{empty} \leq 3.33 \text{ mA}$ and $I_{full} \leq 400 \text{ mA}$.
- R_1 , R_2 and R_4 can now be selected using $V_{reg} = V_{ref}(1 + \frac{R_4}{R_2}) \approx 7.56 \text{ V}$ and $R_o = R_1(1 + \frac{R_4}{R_2}) > 3 \Omega$. Now, $\frac{R_4}{R_2} = 5.05$ and $R_1 = 0.496 \Omega$. Choose $R_1 = 1 \Omega || 1 \Omega$. Choose $R_4 = 270 \Omega$ and $R_2 = 1.5 \text{ k}\Omega || 15 \text{ k}\Omega$ so that $V_{reg} = 7.56 \text{ V}$

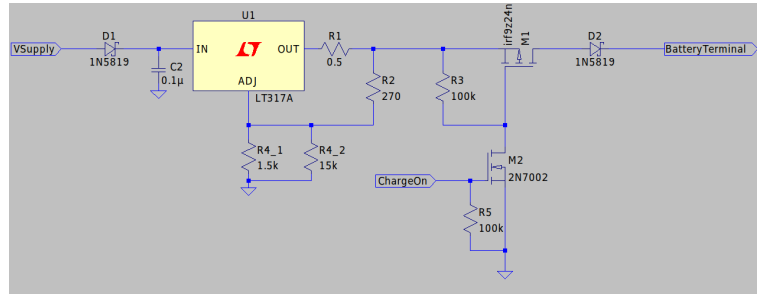


Figure 2.13: Battery Charger Circuit Diagram

2.10. Battery Reader

2.10.1. Configuration

A differential amplifier with a constant negative offset voltage will be used. This circuit will take the raw battery voltage as input, and output a voltage at a scaled-down value that the ESP can read. The circuit diagram can be found in Figure 2.14. A reference voltage of 5 V will be divided using two resistors and pass through a buffer to be used as a negative offset for the circuit.

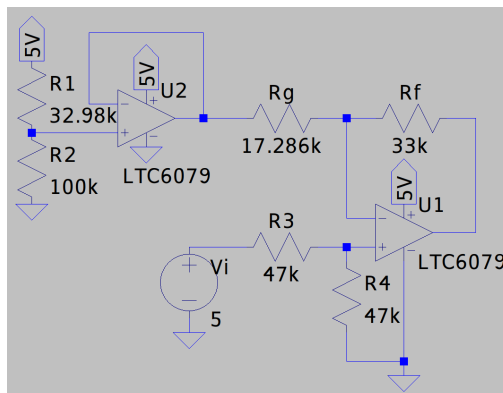


Figure 2.14: Battery Reader Circuit Diagram

2.10.2. Input and Output Range

The input range is a voltage between 5.0 and 7.2 V, and the output is a voltage between 0.1 and 3.3 V. The common-mode input voltage of the op-amp should be taken into account, meaning a voltage divider should be used at the positive input. Without a voltage divider, the battery voltage would be connected directly to the positive terminal of the op-amp, and would be around 7.2 V, which would violate the common-mode specification for the MCP [2]. A voltage divider will therefore first half the voltage, changing the input voltage to be between 2.5 to 3.6 V.

2.10.3. Design

Resistor values may now be calculated:

- The gain of the circuit $m = \frac{3.3V - 0.1V}{3.6V - 2.5V} = 2.91 \text{ V/V} = 1 + \frac{R_f}{R_g}$. To limit current in the feedback loop, ensure $\frac{3.3V}{R_f + R_g} < 100 \mu\text{A} \therefore R_f + R_g > 33 \text{ k}\Omega$. Choose $R_f = 33 \text{ k}\Omega \therefore R_g = 17.286 \text{ k}\Omega$. In order to adjust the gain, use a potentiometer and let $R_g = 15 \text{ k}\Omega + 4.7 \text{ k}\Omega\text{pot}$.
- To minimize current through the positive input voltage divider, ensure $\frac{7.2V}{R_3 + R_4} < 100 \mu\text{A} \therefore R_3 + R_4 > 72 \text{ k}\Omega$. Choose $R_3 = R_4 = 47 \text{ k}\Omega$.
- If the voltage from the divider containing R_1 and R_2 is V_{ref} , then when $V_p = V_n = V_{in} = 2.5 \text{ V}$ and $V_{out} = 0.1 \text{ V}$, $\frac{V_n - V_{ref}}{R_g} + \frac{V_n - V_{out}}{R_f} = 0$ (found using a KCL) $\therefore V_{ref} = 3.76 \text{ V}$.
- Lastly, to calculate resistors R_1 and R_2 , $V_{ref} = 3.76 \text{ V} = 5 \text{ V} \times \frac{R_2}{R_1 + R_2}$. Again, to limit current, choose $R_2 = 100 \text{ k}\Omega \therefore R_1 = 32.98 \text{ k}\Omega$. To adjust this offset voltage, choose $R_1 = 27 \text{ k}\Omega + 10 \text{ k}\Omega\text{pot}$.

2.11. Under-Voltage Protection

2.11.1. Configuration

In order to protect the circuit from drawing too much current when the battery voltage is low, under-voltage protection will be employed. A schmitt trigger will be used to detect when the battery voltage crosses over a specific threshold range. If the voltage drops lower than a specified value, the circuit will remove power from the two motors using a high-side PMOS switch. As soon as the voltage rises above a slightly higher but specified value, the circuit will turn on power to the motors again.

The schmitt trigger will be non-inverting and will use a fixed voltage on the negative terminal as comparator reference. This fixed voltage will be supplied via 5 V and will be divided down using two resistors. Its output will then pass through an NMOS-PMOS combination to ultimately act as a high-side switch for the two motors.

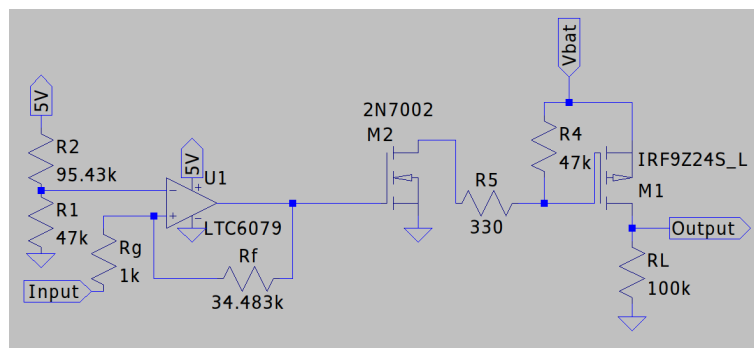


Figure 2.15: Under-Voltage Protection Circuit Diagram

2.11.2. Input Range

The input to the circuit will be the output of the battery reader voltage with a range from 0.1 to 3.3 V. The battery voltage is not used directly, as a fixed voltage is needed as a reference for the schmitt trigger. Since only 3.3 V or 5 V are available (the battery voltage is constantly changing), the crossover point can be maximum 5 V. The choice of using the battery reader voltage also has the benefit of a wider range for the schmitt trigger. The PMOS should therefore switch on when $V_i > 1.45 \times 6 \text{ V} - 7.17 = 1.555 \text{ V}$ and switch off when $V_i < 1.7 \text{ V}$.

2.11.3. Design

First, a KCL can be done at the positive terminal to show that $V_+ = \frac{R_f}{R_f + R_g}V_i + \frac{R_g}{R_f + R_g}V_o$. When this voltage is greater than the voltage at the negative terminal, V_- or V_{ref} , then the op-amp will saturate at the positive rail. Conversely, the op-amp will saturate if $V_+ < V_{ref}$.

It can further be calculated that $V_i = V_+ + \frac{R_g}{R_f}(V_+ - V_o)$. If $V_{o(sat,high)} = 5 \text{ V}$ and $V_{o(sat,low)} = 0 \text{ V}$, resistor values can then be calculated:

- The lower threshold voltage is given as 3 V. This gives the equation at which the output starts to saturate at the negative rail when already saturated at the positive rail. For this case, $1.555 \text{ V} = V_{ref} + \frac{R_g}{R_f}(V_{ref} - 5 \text{ V})$.
- Similarly, the upper threshold voltage gives $1.7 \text{ V} = V_{ref} + \frac{R_g}{R_f}V_{ref}$.
- Solving the above equations simultaneously yields $V_{ref} = 1.652 \text{ V}$ and $\frac{R_g}{R_f} = 0.029$.
- For V_{ref} , choose $R_1 = 47 \text{ k}\Omega$ therefore $R_2 = 95.252 \text{ k}\Omega$. Choose $R_2 = 82 \text{ k}\Omega + 47 \text{ k}\Omega\text{pot}$.
- For R_f and R_g , $\frac{R_g}{R_f} = 0.029$. Choose $R_g = 1 \text{ k}\Omega$ and $R_f = 34.483 \text{ k}\Omega$, with $R_f = 27 \text{ k}\Omega + 10 \text{ k}\Omega\text{pot}$.

2.12. Serial Communication

A serial communication protocol and procedure will be implemented that will allow control of the car, as well as telemetry readings. The protocol will be implemented both over UART and Bluetooth to allow both USB and wireless control. The protocol will set out the rules for communication for a "client" and a "server", including the types of messages and the format of the data. The MCU and PC will then implement this protocol as server and client respectively.

2.12.1. Protocol

Table 2.3 shows the list of messages that may either be sent by the client (a "request"), or sent by the server (a "response"). Each message consists of an ID followed by a potential payload. IDs 000 to 099 are reserved for "get" messages, and 100 to 199 are reserved for "set" messages. *Payload* refers to the data that will be sent be either the client *or* the server. *void* implies that either the client *or* the server must NOT pass any payload for that message. *N/A* implies that either the client *or* the server must NEVER send that message.

Description	ID	Payload (from client)	Payload (from server)
Get All Information	[000]	void	[ID].[Payload] for each "get"
Get Left Wheel Current	[001]	void	[uint4].[uint4] (mA)
Get Right Wheel Current	[002]	void	[uint4].[uint4] (mA)
Get Left Sensor Range	[003]	void	[uint4].[uint4] (mm)
Get Right Sensor Range	[004]	void	[uint4].[uint4] (mm)
Get Battery Voltage	[005]	void	[uint4].[uint4] (mV)
Get Left Wheel Speed	[006]	void	[uint8]
Get Right Wheel Speed	[007]	void	[uint8]
Set Left Wheel Speed	[100]	[uint8]	N/A
Set Right Wheel Speed	[101]	[uint8]	N/A

Table 2.3

Chapter 3

Results

3.1. Voltage Regulation

3.1.1. Measured

As mentioned in the design section, feedback resistors need to be chosen. According to [27], R_2 in Figure 2.3 can be calculated using $V_{out} = V_{ref}(1 + \frac{R_2}{R_1})$. With $V_{out} = 5\text{ V}$, $V_{ref} \approx 1.25\text{ V}$, and $R_1 = 120\Omega$, $R_2 = R_1 \cdot \left(\frac{V_{out}}{V_{ref}} - 1\right) = 360\Omega$. A 470Ω potentiometer was used for the practical circuit to adjust the output to exactly 5 V.

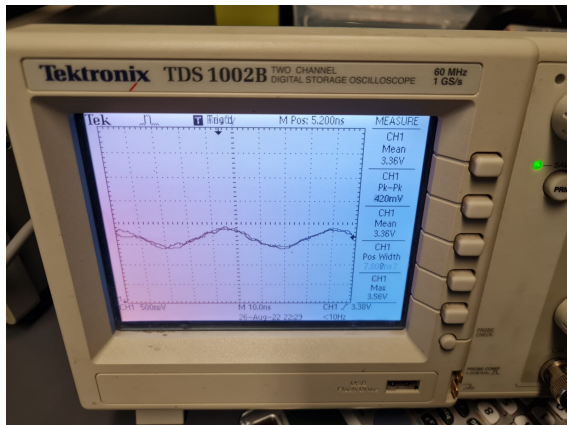


Figure 3.1: 3.3 V Regulator Ripple Measurement

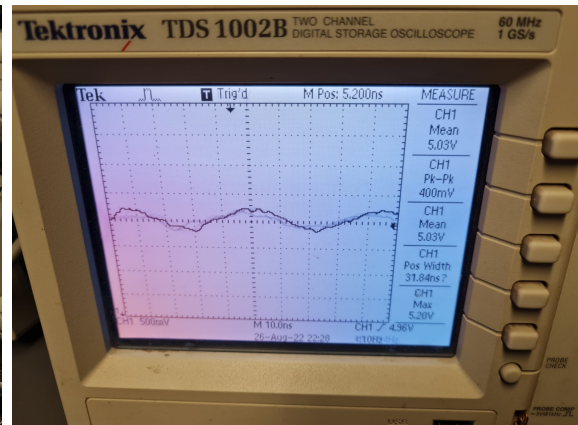


Figure 3.2: 5 V Regulator Ripple Measurement

The ripple in the above figures was measured under full motor load with the worst-case results being shown. Although these results are rather large ($\approx 200\text{ mV}$ deviation from the regulated value), the nominal deviation was less than 50 mV.

3.2. Current Sensor

3.2.1. Simulated

After running initial simulations, it was clear that the constant assumed in the design stage for the dominant capacitor C_f was too high. The capacitor value was then experimentally increased to 100nF where a satisfactory response which was reasonably below 250 mV (10-20%) was obtained. This section details the rest of the results of these simulations.

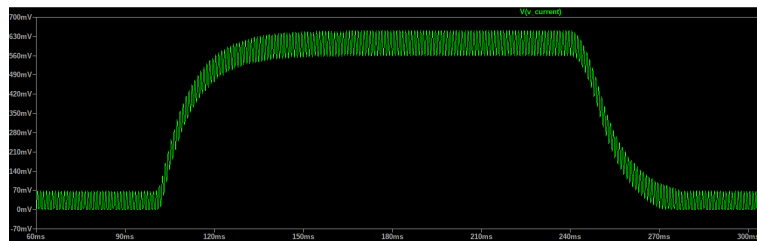


Figure 3.3: Output and Noise Level in Response to Step Input

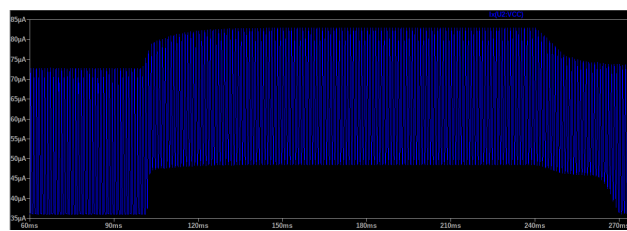


Figure 3.4: Current Draw

As can be seen, all specifications were adhered to:

- The noise level at idle is well below the 250 mV requirement.
- The step response input changes 20-25 ms, which is below the 100 ms requirement.
- The power draw of the circuit (as measure at the positive terminal of the op-amp) is less than 85 uA, which is much less than the specified 150 uA.

Lastly, the input simulation parameters were modified during testing to analyze the various output voltages for different input currents. For input currents of 400mA, 500mA, 800mA and 1A, the output voltages were 1.22V, 1.52, 2.43 and 3.024 V respectively. This matches perfectly with the initial design.

3.2.2. Measured

Tests were conducted with a function generator to ensure the amplifier met specifications.

As can be seen in Figure 3.5, the amplifier noise requirement was satisfied. The input signal (channel 1, bottom) is a 10 mV_{pp} 1 kHz sine wave with 6 mV offset. It is required that

a sinusoidal "noise" signal greater than this frequency should not be amplified to more than 250 mV_{pp}. An output of 1.13 V - 0.949 V = 181 mV was obtained - within the threshold.

In Figure 3.6, the amplifier's step response time was recorded as 4.957 ms, which is much below the 100 ms requirement. This time is 4x better than the designed/simulated circuit, presumably due to the increased resistance value and other tolerances.

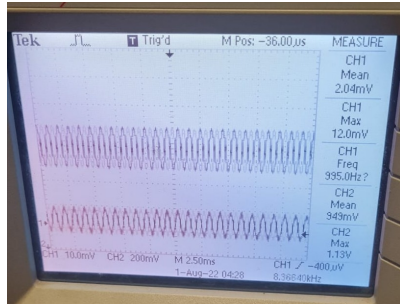


Figure 3.5: Noise Level

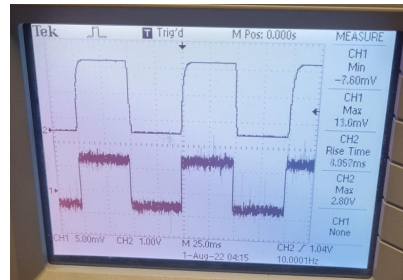


Figure 3.6: Step Response

Current measurements were then made with the motor connected, as visible in Table 3.1. As can be analyzed, there is an offset voltage of 0.42 V at the output. The actual gain can be calculated as e.g. $\frac{1.42\text{ V} - 0.42\text{ V}}{210\text{ mA} * 10\text{ m}\Omega} = 476\text{ V/V}$. With the 120 kΩ resistor, an ideal gain of $\frac{120\text{ k}\Omega}{330\text{ }\Omega} = 363.6\text{ V/V}$ was expected, however due to the nature of the circuit (which contains 4 resistors) a tolerance of 10% * 4 should be accounted for, which explains the higher gain.

Motor Condition	PSU Current (mA)	Output Voltage (V)
Stall	1200	3.31
Slight Load	305	1.96
Free Running	210	1.42
I = 150 mA	150	1.13
I = 100 mA	100	0.91
I = 50 mA	50	0.63
I = 0 mA	0	0.42

Table 3.1: Measurements of Motor Current and Voltage

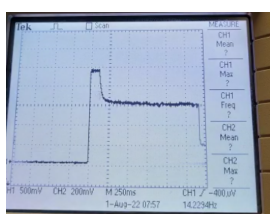


Figure 3.7: Open Circuit to Free Running

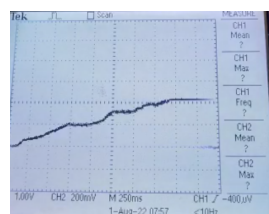


Figure 3.8: Increasing Load

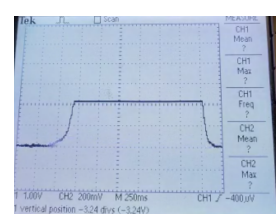


Figure 3.9: Free Running to Stall

3.3. Range Sensor

3.3.1. Simulated

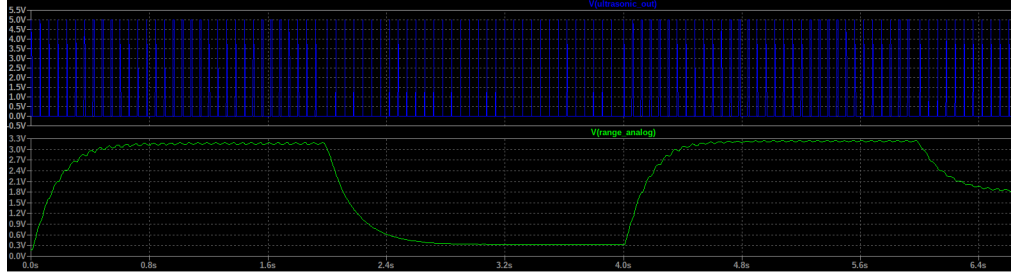


Figure 3.10: Full-Range PWM using Modified Workbench

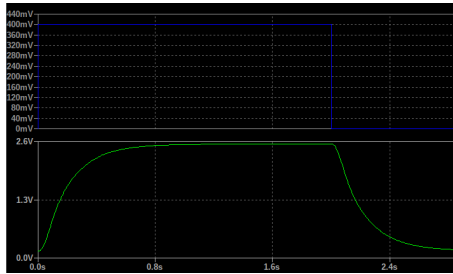


Figure 3.11: 400 mV Step Response
Input vs Output

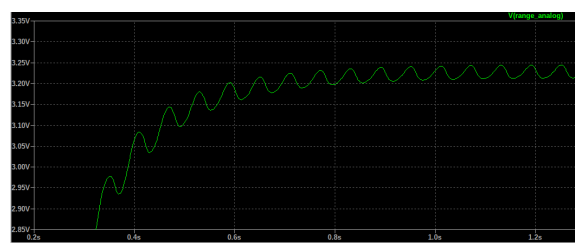


Figure 3.12: Noise Level

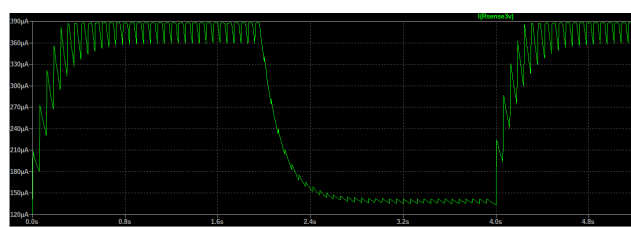


Figure 3.13: Current Draw

As seen in the above figures, all specifications were complied with:

- Figure 3.10 demonstrates the default simulation to test the distance limits with $\tau = 0.05\%$ to 9.5% , followed by the original workbench settings. As visible, the output is ≥ 3.0 V for far distances, and ≤ 300 mV for close distances.
- Figure 3.11 shows the response time of around 800 ms, much less than required 1.5 s.
- Figure 3.12 demonstrates the low noise ripple of around 50 mV, less than the required 70 mV.
- Figure 3.13 indicates a maximum current draw of 390 μ A, less than the maximum 750 μ A.

3.3.2. Measured

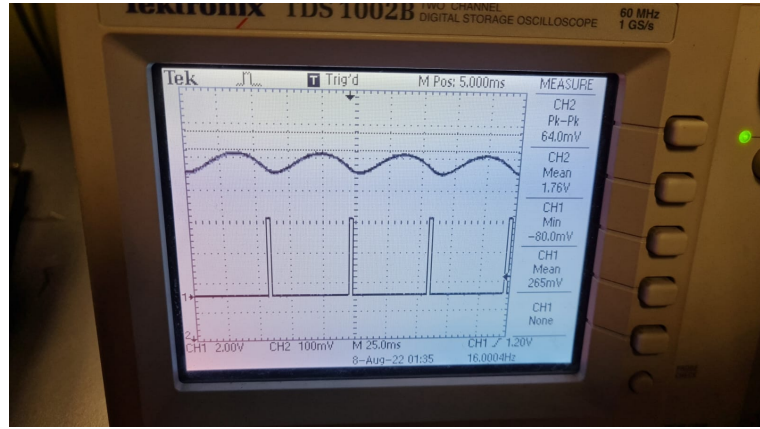


Figure 3.14: Noise Level

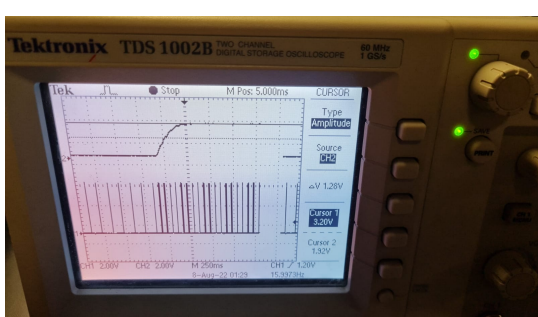


Figure 3.15: Step Response

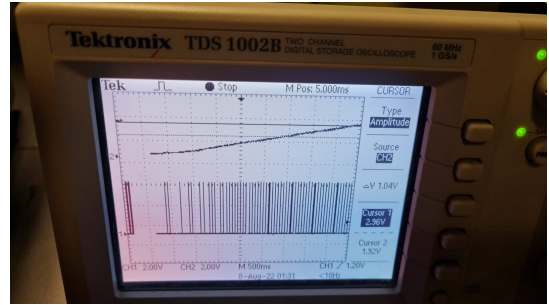


Figure 3.16: Gradual Change over Input Range

Similarly, the implementation of the circuit also complied with specifications:

- Figure 3.14 indicates a noise level of $64 \text{ mV}_{\text{pp}}$. Although this is only measured at 1.76 V output, it seems the oscilloscope was struggling to provide accurate readings and could not be zoomed in further.
- Figure 3.15 indicates a rise time of around 300 ms.
- Figure 3.16 shows the gradual response of the circuit. The cursor is on 2.96 V in the Figure, and by counting divisions it can be seen that it began at around 0.2 V . This shows a relatively linear response.

3.4. Digital to Analog Converter

3.4.1. Simulated

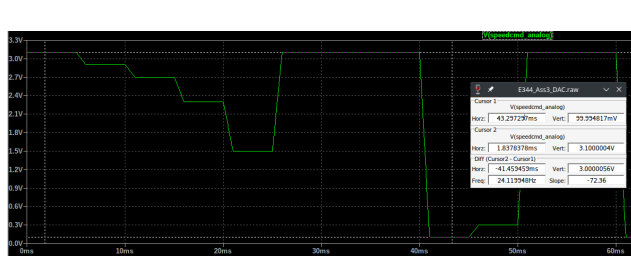


Figure 3.17: Output Range from 0000 (First Cursor) to 1111 (Second Cursor)

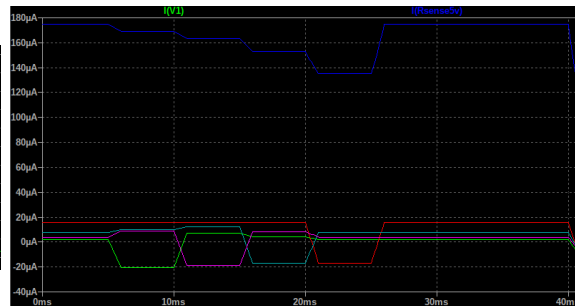


Figure 3.18: Current Draw (Amplifier and Digital Inputs)

As seen in the above figures, all specifications were complied with:

- Figure 3.17 shows that an output of 0000 produces exactly 3.1 V on the output, and that 1111 produces 100 mV.
- Figure 3.18 shows a maximum current draw of under 180 μ A, which is much under the 250 μ A specification. It also shows that each digital input draws less than 20 μ A, also under the 50 μ A specification.

3.4.2. Measured

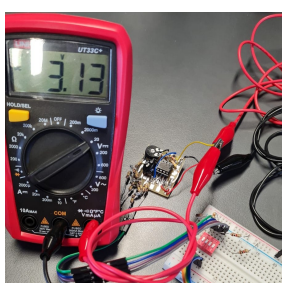


Figure 3.19:
DAC Output
at 0000

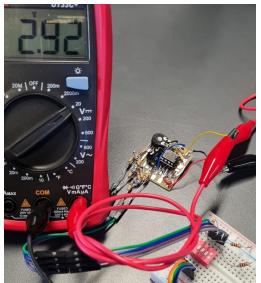


Figure 3.20:
DAC Out-
put at 0001

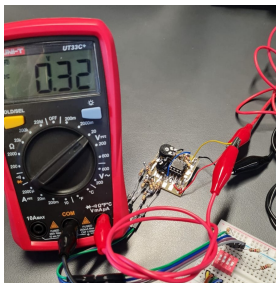


Figure 3.21:
DAC Output
at 1110

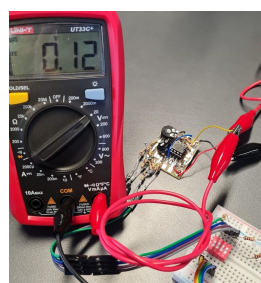


Figure 3.22:
DAC Out-
put at 1111

Figures 3.19 to 3.22 demonstrate the output voltages at specific digital input combinations. All specifications are complied with, specifically that 0000 produces > 3 V on the output, and that 1111 produces < 0.5 V.

3.5. Analog Motor Controller

3.5.1. Simulated

The results of the simulation for the two motor controller stages can be found below.



Figure 3.23: Motor Controller Output of Subtractor Stage



Figure 3.24: Motor Controller Current Draw of Subtractor Stage

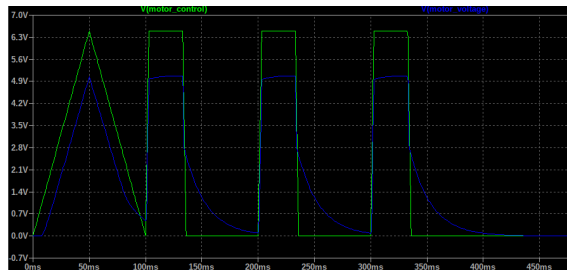


Figure 3.25: Motor Controller Output of Power Stage

As can be seen, specifications were complied to:

- A "low speed" command (3 V) and "no object" command (3 V) results in a low controller command (< 1.8 V).
- A "high speed" command (0.5 V) and "no object" command (3 V) results in a high controller command. The output, however, only reaches 6 V due to a different input range. A simulation with $V_{speed} = 0.1$ V and $V_{range} = 3.3$ V shows that the output saturates at 7.2 V.
- The current draw of the subtractor is as designed i.e. < 400 μ A, and therefore the total current is < 1.5 A due to the maximum motor current draw of 1 A.
- The drop from the motor control command to the motor is 1.4 V, meaning the designed minimum of 1.8 V will ensure the motor has $V_{motor} < 0.5$ V.

3.5.2. Measured

Voltage measurements over the motor for the four edge-cases of the motor controller can be seen below.

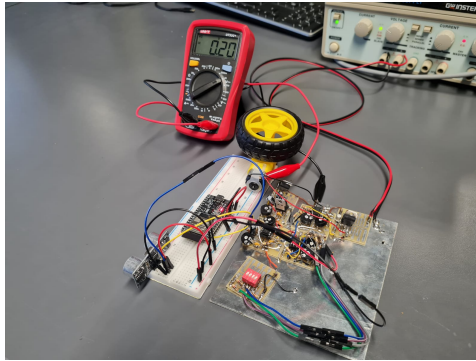


Figure 3.26: Motor Voltage:
Object Far, Speed 0000

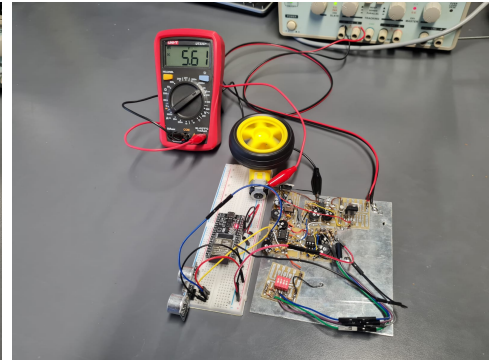


Figure 3.27: Motor Voltage:
Object Far, Speed 1111

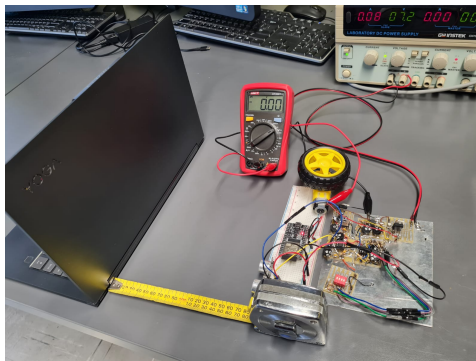


Figure 3.28: Motor Voltage:
Object Near, Speed 0000

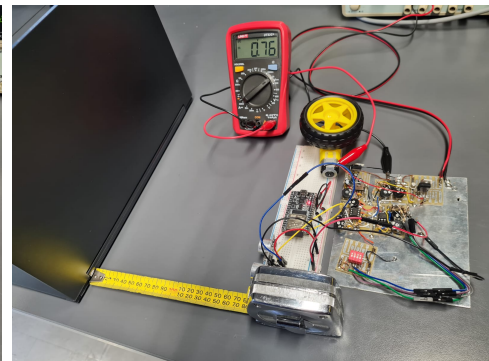


Figure 3.29: Motor Voltage:
Object Near, Speed 1111

The above four conditions show that the requirements were adhered to, in that the voltage is high > 5.5 V when the object is far and the torque command is a maximum, and the voltage is low < 0.5 V in all other edge-cases.

The designed 20 cm threshold was also measured, with the voltage resultant being 0.76 V as shown in Figure 3.30. Although this was designed to equal 0.6 V at 20 cm, the motor is switched off at 0.76 V, and so the final requirement was still met.

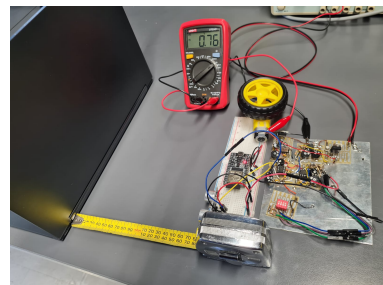


Figure 3.30: Motor Voltage: Object 20cm, Speed 1111

3.6. Digital Motor Controller

3.6.1. Simulated

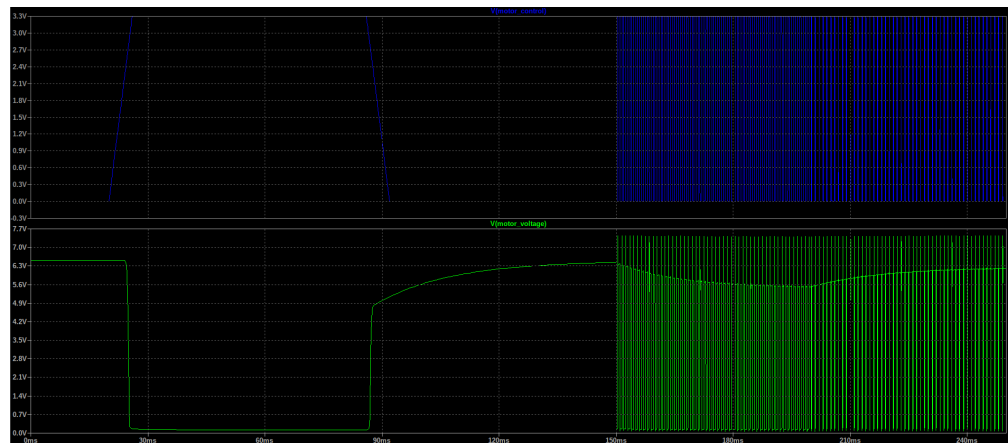


Figure 3.31: Motor Output Voltage vs Motor Control

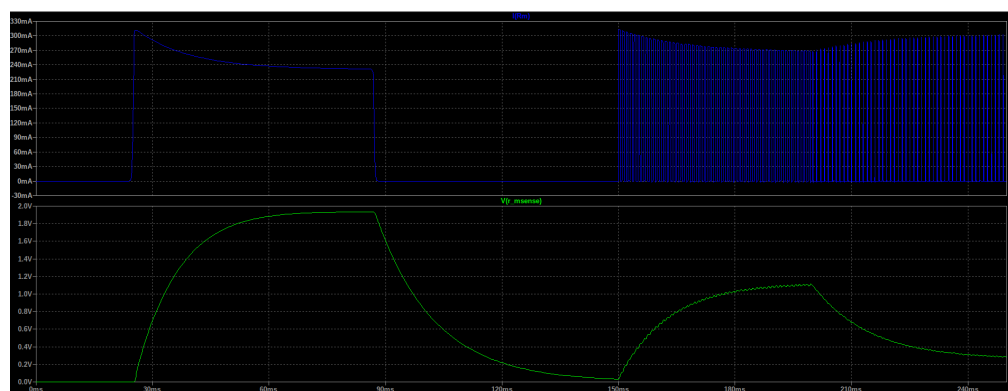


Figure 3.32: Motor Current vs Current Sensor Output



Figure 3.33: MOSFET Turn On Time vs Motor Control

3.6.2. Measured

The following figures display the current sensor and PWM control output for different combinations of DAC and range sensor conditions.



Figure 3.34: Object Far, DAC 1111

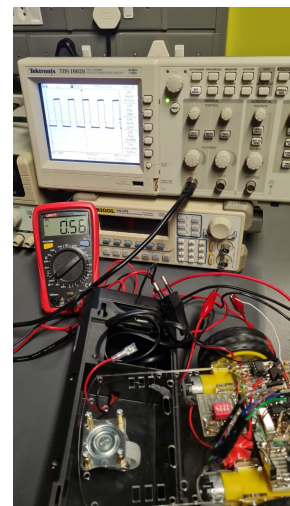


Figure 3.35: Object Far, DAC 0000

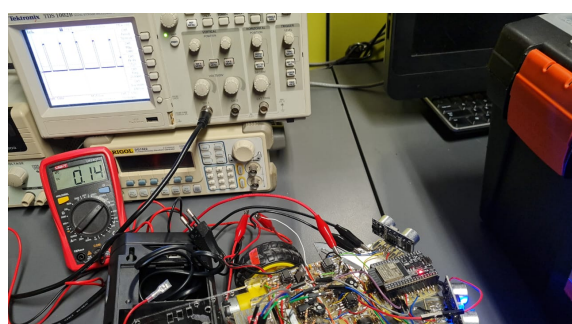


Figure 3.36: Object Near, DAC 1111

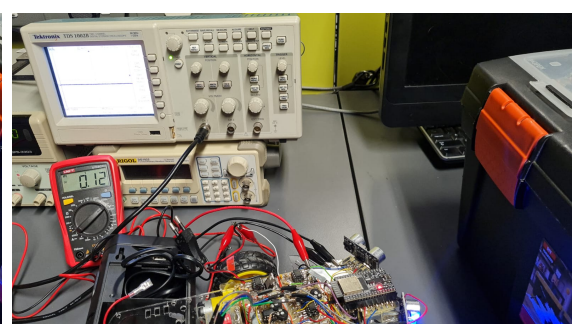


Figure 3.37: Object Near, DAC 0000

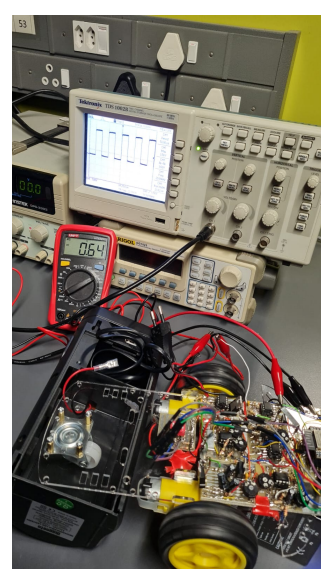


Figure 3.38: Object 50cm, DAC 1111

3.7. Battery Charger

3.7.1. Simulated

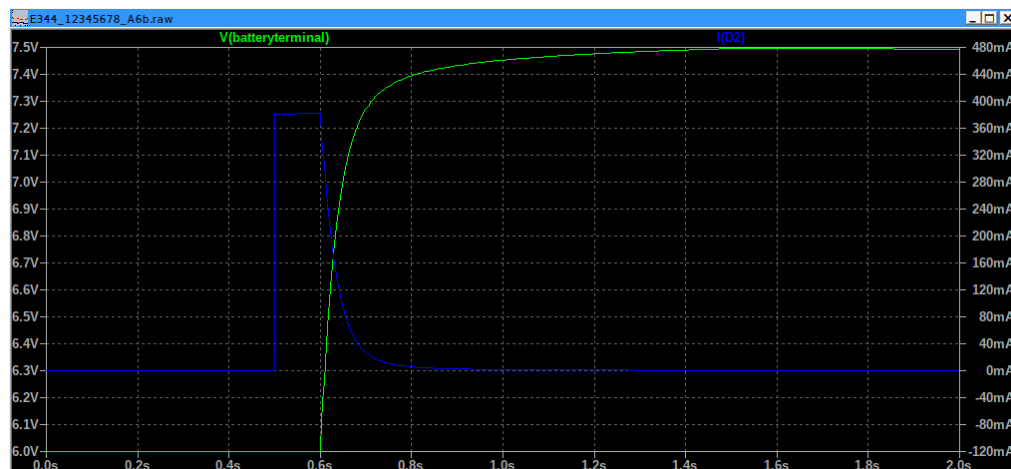


Figure 3.39: Batter Charger Final Voltage and Current

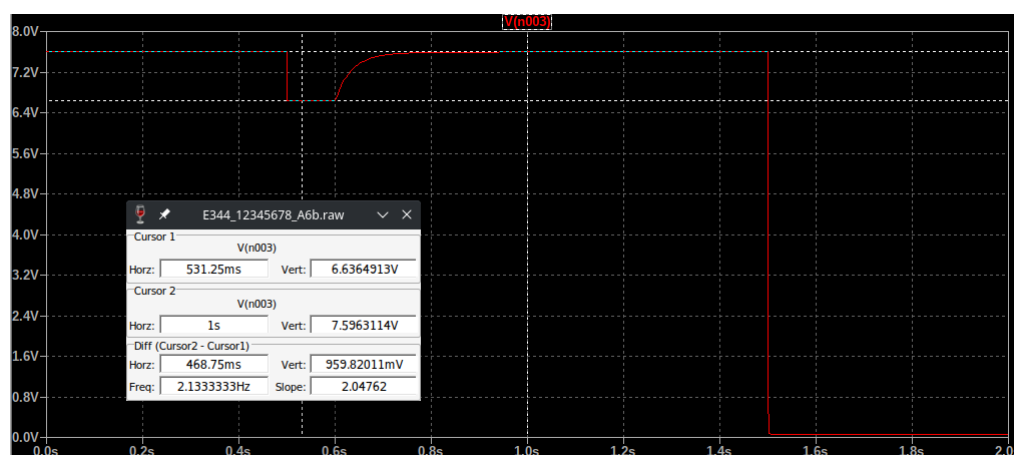


Figure 3.40: Battery Charger Internal Voltage Regulation vs Changing Load

3.7.2. Measured

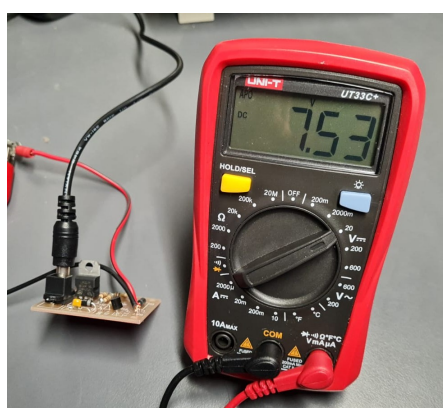


Figure 3.41: Battery Charger No-Load Voltage

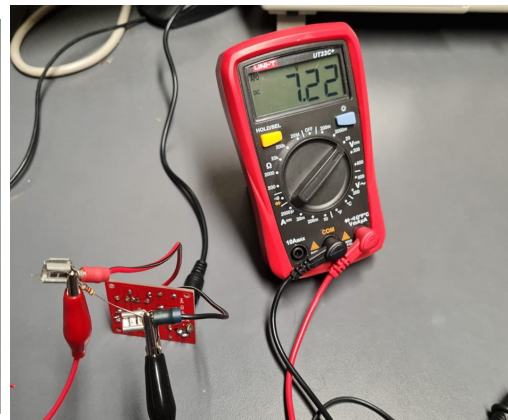


Figure 3.42: Battery Charger Voltage with $1\text{ k}\Omega$ Load

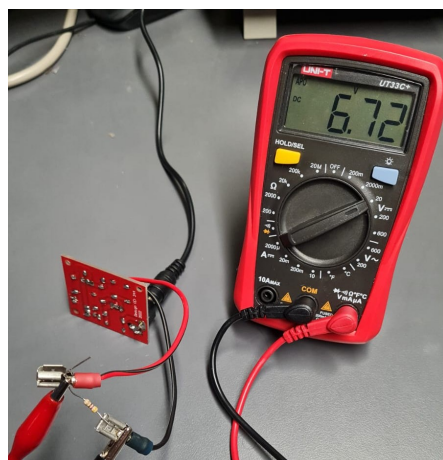


Figure 3.43: Battery Charger Voltage with $50\ \Omega$ Load

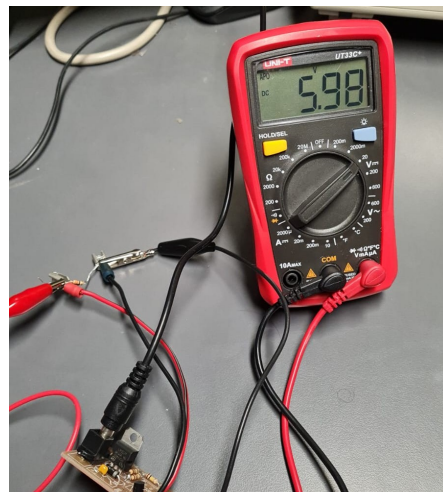


Figure 3.44: Battery Charger with $15\ \Omega$ Load (approx. uncharged battery)

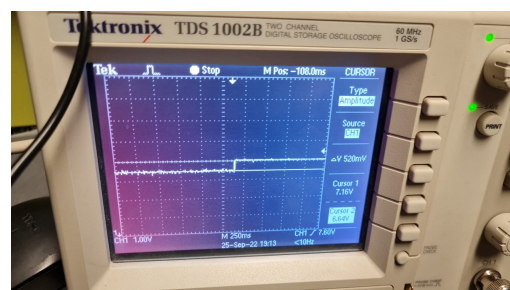


Figure 3.45: Battery Charger Voltage Regulation under Changing Load

3.8. Battery Reader and Under-Voltage Protection

3.8.1. Simulated



Figure 3.46: Battery Reader Output vs 5.0 to 7.2 V Input

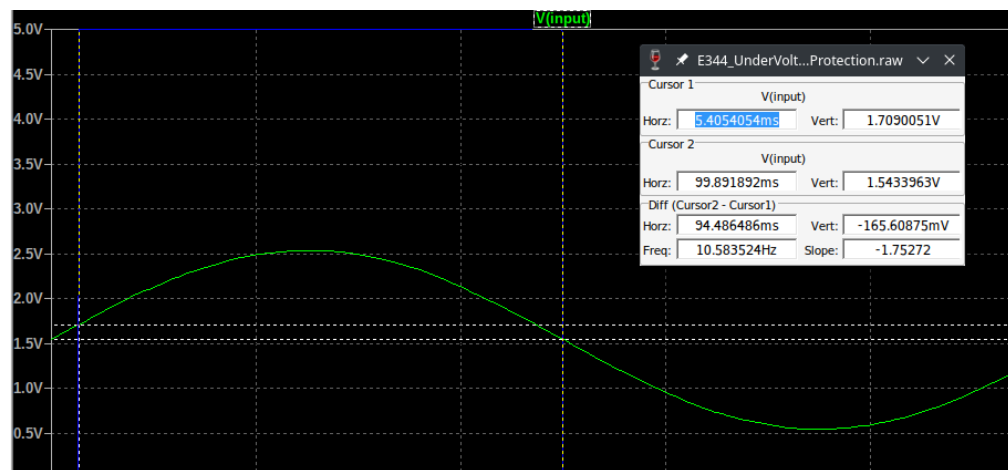


Figure 3.47: Under-Voltage Scmitt Trigger Output vs Sine Wave Input

3.8.2. Measured



Figure 3.48: Battery Reader at 7.2 V

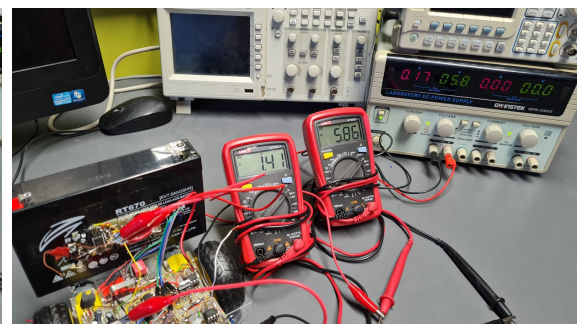


Figure 3.49: Battery Reader at 5.9 V

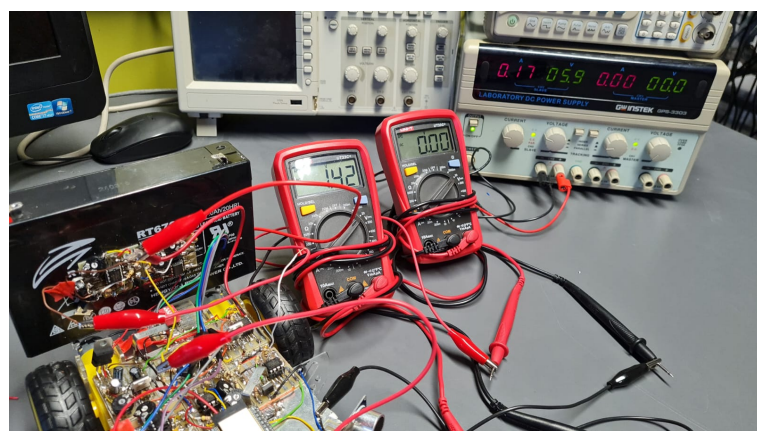


Figure 3.50: Battery Reader at 5.9 V with Under-Voltage Protection Battery Voltage

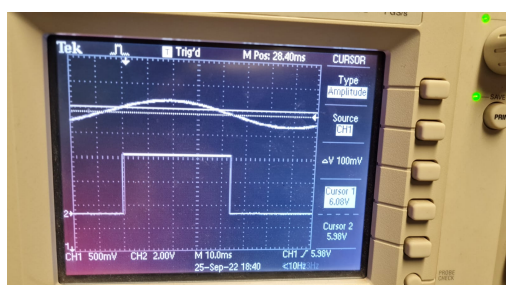


Figure 3.51: Under-Voltage Protection Output of Schmitt Trigger

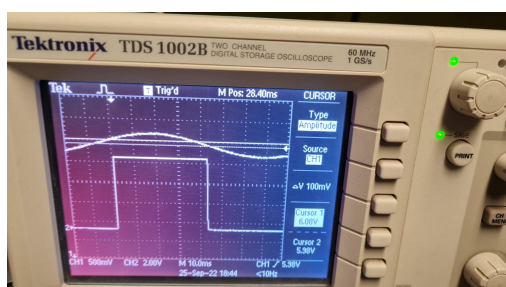


Figure 3.52: Under-Voltage Protection Output of Battery Voltage

Chapter 4

Physical Implementation

4.1. Combined Circuit

The final combined circuit can be found below, with the individual components labeled appropriately.

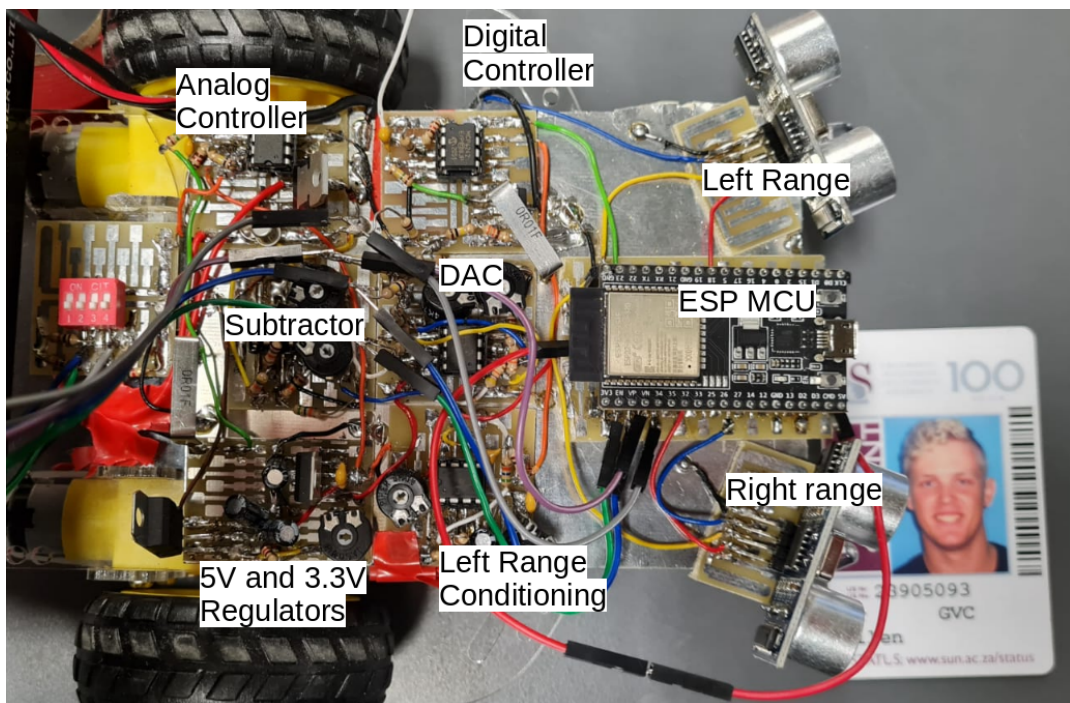


Figure 4.1: Final Combined Circuit

4.2. Current Sensor

The implementation of the circuit was different in two ways compared to the original design:

- 120 k Ω resistors were used instead of 100 k Ω , as they were easier to obtain, and would only result in a slightly larger gain and lower cutoff.
- The amplifier circuit was powered with regulated 3.3 V. This was done to protect the ESP's input pins by saturating the output when it would have been too large.

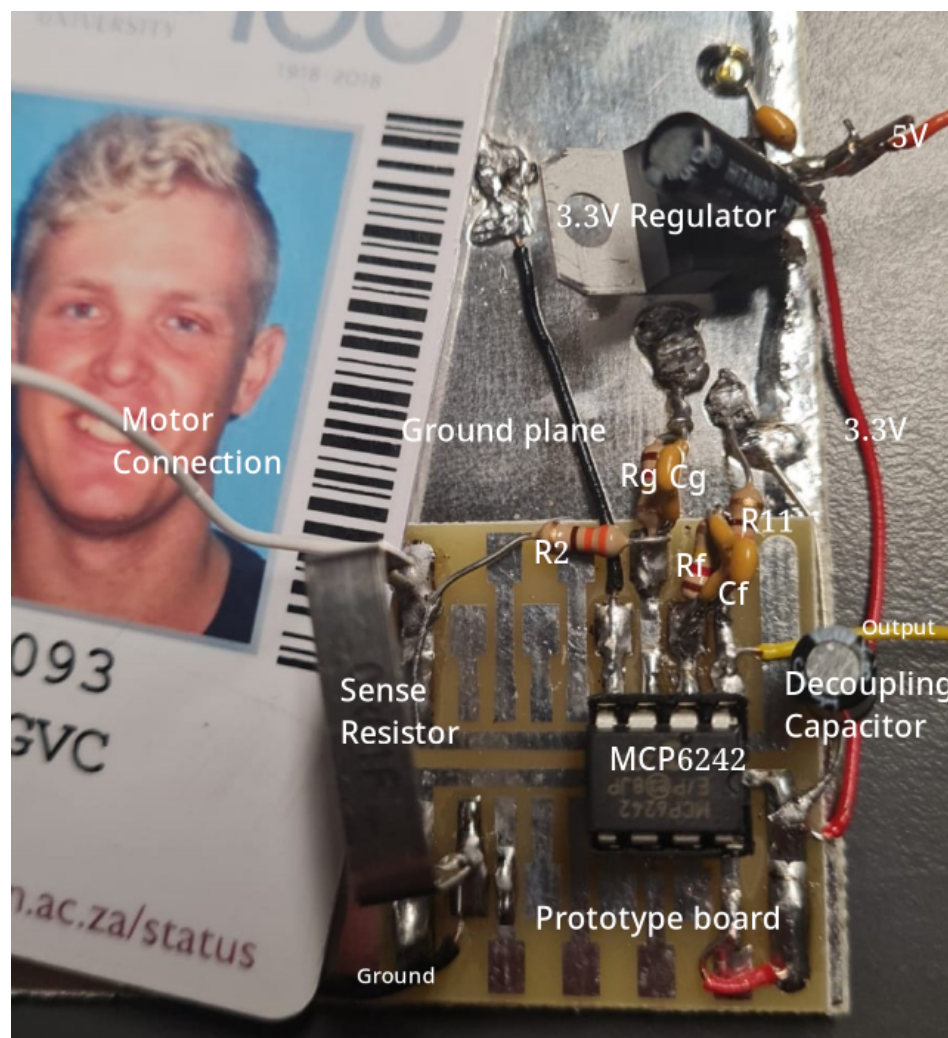


Figure 4.2: Current Sensor Physical Circuit

4.3. Range Sensor



Figure 4.3: Ultrasonics Sensor Amplifier Physical Circuit

4.4. Digital to Analog Converter



Figure 4.4: Digital to Analog Converter Physical Circuit

Bibliography

- [1] Tutorials Point, “Physical limitations of operational amplifiers.” [Online]. Available: <https://www.tutorialspoint.com/physical-limitations-of-operational-amplifiers>
- [2] Microchip, “Mcp6241/1r/1u/2/4.” [Online]. Available: <https://ww1.microchip.com/downloads/aemDocuments/documents/OTH/ProductDocuments/DataSheets/21882d.pdf>
- [3] Elec Freaks, “Ultrasonic ranging module hc - sr04.” [Online]. Available: <https://cdn.sparkfun.com/datasheets/Sensors/Proximity/HCSR04.pdf>
- [4] STMicroelectronics, “Tip31c power transistors.” [Online]. Available: <https://www.st.com/content/ccc/resource/technical/document/datasheet/a2/01/d8/6b/ba/9d/49/86/CD00104632.pdf/jcr:content/translations/en.CD00104632.pdf>
- [5] WikiBooks, “Op amp configurations.” [Online]. Available: <https://ww1.microchip.com/downloads/aemDocuments/documents/OTH/ProductDocuments/DataSheets/21882d.pdf>
- [6] ElectronicsTutorials, “Second order filters.” [Online]. Available: <https://www.electronics-tutorials.ws/filter/second-order-filters.html>
- [7] HiokiUSA, “6 current sensing methods.” [Online]. Available: <https://hiokiusa.com/6-current-sensing-methods/>
- [8] AllAboutCircuits, “Low side vs high side sensing.” [Online]. Available: <https://www.allaboutcircuits.com/technical-articles/resistive-current-sensing-low-side-versus-high-side-sensing/>
- [9] Engineering360, “How electric current sensor technology works,” 5 2015. [Online]. Available: <https://insights.globalspec.com/article/994/how-electric-current-sensor-technology-works>
- [10] AllAboutCircuits, “Logic signal voltage levels.” [Online]. Available: <https://www.allaboutcircuits.com/textbook/digital/chpt-3/logic-signal-voltage-levels/>
- [11] M. Mohamed, A. Elmahalawy, and H. Harb, “Developing the pulse width modulation tool (pwmt) for two timer mechanism technique in microcontrollers,” pp. 148–153, 12 2013.
- [12] Microchip, “Using pwm to generate an analog output,” 2020. [Online]. Available: <http://ww1.microchip.com/downloads/en/Appnotes/90003250A.pdf>

- [13] PeopleECE, “First-order system example.” [Online]. Available: https://people-ece.vse.gmu.edu/~gbeale/ece_421/xmpl-421-1st-order-01.pdf
- [14] M. Gopal, *Digital Control and State Variable Methods: Conventional and Neural-fuzzy Control Systems*. Tata-McGraw Hill, 2003. [Online]. Available: <https://books.google.co.za/books?id=L4W491WeR0oC>
- [15] Inductiveload, Wikipedia. [Online]. Available: <https://commons.wikimedia.org/w/index.php?curid=5786242>
- [16] H. Wallman, *Transient response and the central limit theorem of probability*. Taub, A. H., 1950.
- [17] Texas Instruments, “Active filter design techniques,” 2001. [Online]. Available: <https://web.archive.org/web/20060616013258/http://focus.ti.com/lit/ml/sloa088/sloa088.pdf>
- [18] Bruce Carter, “Designing gain and offset in thirty seconds,” 2002. [Online]. Available: <https://www.ti.com/lit/an/sloa097/sloa097.pdf>
- [19] element14, “How do ultrasonic distance sensors work?” 2021. [Online]. Available: <https://www.youtube.com/watch?v=2ojWO1QNprw>
- [20] Mubina Toa, Akeem Whitehead, “Ultrasonic sensing basics,” 2022. [Online]. Available: <https://www.ti.com/lit/an/slaa907d/slaa907d.pdf>
- [21] Peter Vis, “4 bit dac using op-amp - example 2.” [Online]. Available: <https://www.petervis.com/Education/summing-amplifier-inverting/4-bit-dac-using-op-amp-example-2.html>
- [22] w2aew, “140: Basics of an op amp summing amplifier.” [Online]. Available: <https://www.youtube.com/watch?v=juQtVIx1a8g>
- [23] Tony R. Kuphaldt, “The r2r dac (digital-to-analog converter),” 2021. [Online]. Available: <https://www.youtube.com/watch?v=juQtVIx1a8g>
- [24] Espressif, “Esp32-wroom-32d & esp32-wroom-32u datasheet.” [Online]. Available: https://www.espressif.com/sites/default/files/documentation/esp32-wroom-32d_esp32-wroom-32u_datasheet_en.pdf
- [25] Adrian S. Nastase, “A summing and differential amplifier with one op amp.” [Online]. Available: <https://masteringelectronicsdesign.com/a-summing-and-differential-amplifier-with-one-op-amp/>
- [26] ON Semiconductor, “P2n2222a amplifier transistors.” [Online]. Available: <https://www.onsemi.com/pdf/datasheet/p2n2222a-d.pdf>

- [27] ST Microelectronics, “Ld1117 - adjustable and fixed low drop positive voltage regulator.” [Online]. Available: <https://www.st.com/content/ccc/resource/technical/document/datasheet/99/3b/7d/91/91/51/4b/be/CD00000544.pdf/files/CD00000544.pdf/jcr:content/translations/en.CD00000544.pdf>
- [28] Fairchild Semiconductor, “Fqd13n06l - 60 v logic n-channel mosfet.” [Online]. Available: <https://docs.rs-online.com/1c55/0900766b80d27f42.pdf>
- [29] Espressif, “Led control (ledc),” 2016. [Online]. Available: <https://docs.espressif.com/projects/esp-idf/en/latest/esp32/api-reference/peripherals/ledc.html>
- [30] Battery University, “Bu 403: Charging lead acid,” 2021. [Online]. Available: <https://batteryuniversity.com/article/bu-403-charging-lead-acid>
- [31] Power-Sonic, “How to charge a lead-acid battery,” 2021. [Online]. Available: <https://www.power-sonic.com/blog/how-to-charge-a-lead-acid-battery/>
- [32] RITAR, “Rt670.” [Online]. Available: <https://www.mantech.co.za/datasheets/products/RT670.pdf>
- [33] International Rectifier, “Irf9z24npbf: Hexfet power mosfet.” [Online]. Available: <https://docs.rs-online.com/519d/0900766b8079172c.pdf>
- [34] Fairchild Semiconductor, “N-channel enhancement mode field effect transistor.” [Online]. Available: <https://docs.rs-online.com/591b/0900766b8145d5d8.pdf>
- [35] STMicroelectronics, “1n5817, 1n5818, 1n5819 low drop power schottky rectifier.” [Online]. Available: <https://www.st.com/content/ccc/resource/technical/document/datasheet/26/db/14/60/52/47/47/5b/CD00001625.pdf/files/CD00001625.pdf/jcr:content/translations/en.CD00001625.pdf>
- [36] ——, “Lm217, lm317: 1.2 v to 37 v adjustable voltage regulators.” [Online]. Available: <https://docs.rs-online.com/0054/0900766b813862fa.pdf>

Appendix A

Social contract



UNIVERSITEIT•STELLENBOSCH•UNIVERSITY
jou kennisvennoot • your knowledge partner

E-design 344 Social Contract

2022

The purpose of this document is to establish commitment between the student and the organisers of E344. Beyond the commitment made here, it is not binding.

In the months preceding the term, the lecturer (Thinus Booyens) and a few paid helpers (Rita van der Walt, Keegan Hull, and Michael Ritchie) spent countless hours to prepare for E344 to ensure that you get your money's worth, that you are enabled to learn from the module, and demonstrate and be assessed on your skills. We commit to prepare the assignments, to set the assessments fairly, to be reasonably available, and to provide feedback and support as best and fast we can. We will work hard to give you the best opportunity to learn from and pass analogue electronic design E344.

I, Gary Allen have registered for E344 of my own volition with the intention to learn of and be assessed on the principals of analogue electronic design. Despite the potential publication online of supplementary videos on specific topics, I acknowledge that I am expected to attend the scheduled lectures to make the most of these appointments and learning opportunities. Moreover, I realise I am expected to spend the additional requisite number of hours on E344 as specified in the yearbook.

I acknowledge that E344 is an important part of my journey to becoming a professional engineer, and that my conduct should be reflective thereof. This includes doing and submitting my own work, working hard, starting on time, and assimilating as much information as possible. It also includes showing respect towards the University's equipment, staff, and their time.

Prof. MJ (Thinus) Booyens

MJ Booyens
Signature:

Date: 1 July 2022

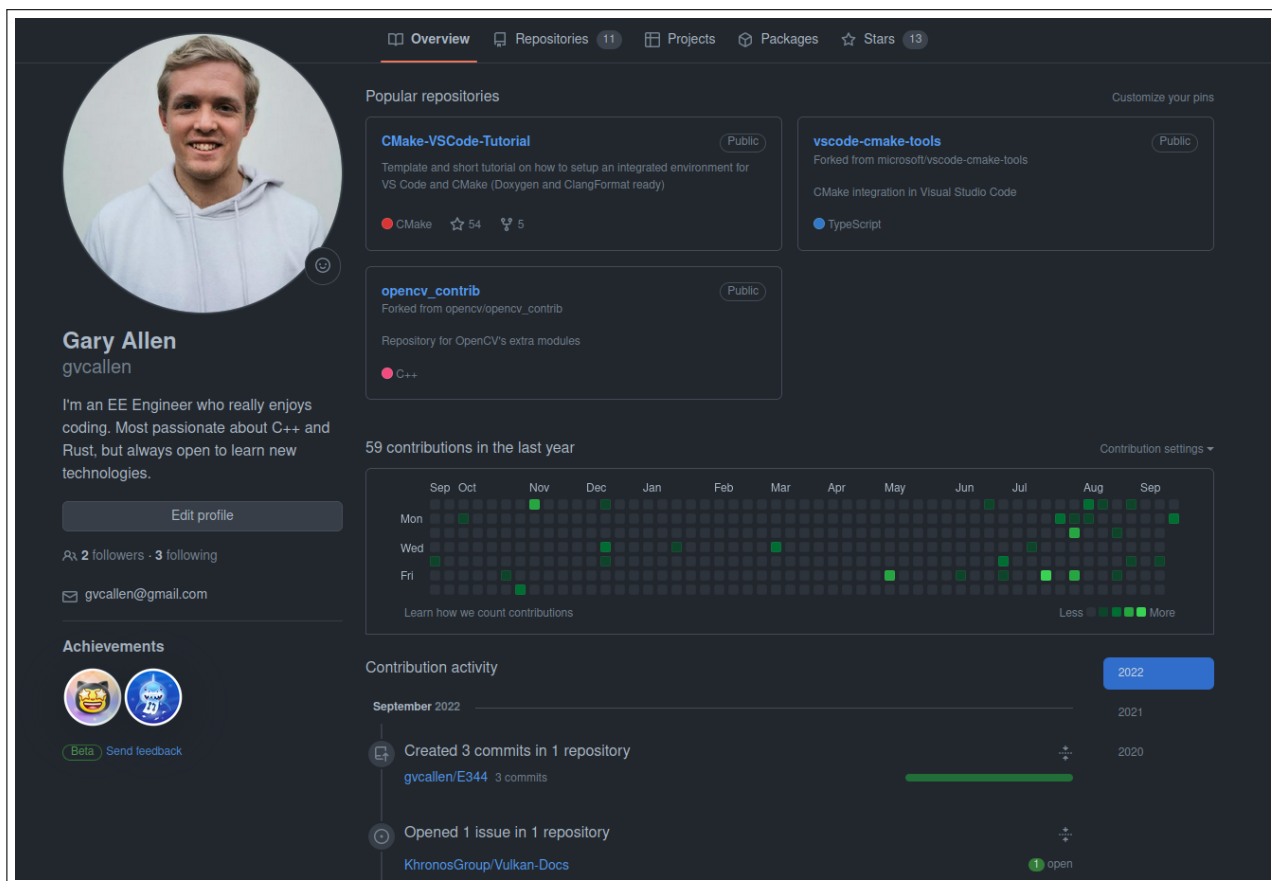
Student number: 2390803

Signature: Dale

Date: 07 / 07 / 2022

Appendix B

GitHub Activity Heatmap



Appendix C

Formulae and Derivations

C.1. Filters

C.1.1. Common Filter Formulae

In the following formulae, f_c is the filter's cutoff frequency, $w_c = 2\pi f_c$, and $H(s)$ is the Laplace transfer function of the filter.

For a 1st order filter:

- $H(s) = \frac{w_c}{s+w_c}$
- Attenuation (dB) = $-10 \log[1 + (\frac{f}{f_c})^2]$ [12]
- 10% to 90% Rise time, $t_r \approx \frac{2.2}{w_c}$ [13]

For a 2nd order filter:

- $H(s) = \frac{w_c^2}{s^2 + 2\zeta w_c s + w_c^2}$
- Attenuation (dB) = $-10 \log[1 + (\frac{f}{f_c})^4]$ with $\zeta = 0.707$ [C.2]
- 10% to 90% Rise time, $t_r \approx \frac{3.3}{w_c}$ with $\zeta = 0.707$ [14]

For a 3rd order filter (formed by cascading a 1st and 2nd order):

- $H(s) = \left(\frac{w_c}{s+w_c}\right) \left(\frac{w_c^2}{s^2 + 2\zeta w_c s + w_c^2}\right)$
- Attenuation (dB) = $-10 \log[1 + (\frac{f}{f_c})^2 + (\frac{f}{f_c})^4 + (\frac{f}{f_c})^6] \approx -60 \log \left[\frac{f}{f_c}\right]$ with $\zeta = 0.707$ and $f >> f_c$.
- 10% to 90% Rise time, $t_r \approx \frac{3.97}{w_c}$ with $\zeta = 0.707$, using $t_{ro} = \sqrt{t_{r1}^2 + t_{r2}^2}$ from [16]

C.1.2. 2nd Order Filter Attenuation

For a 2nd order filter with the following transfer function:

$$H(s) = \frac{w_c^2}{s^2 + 2\zeta w_c s + w_c^2}$$

The attenuation A_{dB} at frequency w can be calculated as follows:

$$\begin{aligned}
A_{dB} &= 20 \log \left| \frac{w_c^2}{(jw)^2 + 2\zeta w_c(jw) + w_c^2} \right| \\
&= -20 \log \left| \frac{(w_c^2 - w^2) + j(w2\zeta w_c)}{w_c^2} \right| \\
&= -20 \log \sqrt{\frac{w_c^4 - 2w_c^2 w^2 + w^4 + 4\zeta^2 w_c^2 w^2}{w_c^2}} \\
&= -10 \log \left[\frac{w_c^4 + w^4}{w_c^4} + \frac{w_c^2 w^2 (4\zeta^2 - 2)}{w_c^4} \right] \\
&= -10 \log \left[1 + \left(\frac{w}{w_c} \right)^4 + \left(\frac{w}{w_c} \right)^2 (4\zeta^2 - 2) \right]
\end{aligned} \tag{C.1}$$

For the case when $\zeta = 0.707$ (i.e. when optimally damped), then C.1 simplifies to:

$$A = -10 \log \left[1 + \left(\frac{w}{w_c} \right)^4 \right] \tag{C.2}$$

C.1.3. 1st and 2nd Order Filter Cutoff vs Attenuation

Given:

- $f_n = f_{\text{cutoff}} (n^{\text{th}} \text{ order})$.
- For 1st order, attenuation (dB) @ $f = -10 \log[1 + (\frac{f}{f_c})^2]$ [12]
- For 2nd order, attenuation (dB) @ $f = -10 \log[1 + (\frac{f}{f_c})^4]$ with $\zeta = 0.707$ [C.2]

A 1st order filter will therefore always attenuate a given frequency f less than a 2nd order filter with $f_1 = f_2$. The cutoff frequency of a 2nd order filter that will attenuate f by the same amount as a 1st order filter with a given cutoff frequency f_1 can be calculated as follows:

$$\begin{aligned}
-10 \log \left[1 + \left(\frac{f}{f_1} \right)^2 \right] &= -10 \log \left[1 + \left(\frac{f}{f_2} \right)^4 \right] \\
\left(\frac{f}{f_1} \right)^2 &= \left(\frac{f}{f_2} \right)^4 \\
\therefore f_2^4 &= \frac{f^4}{f^2} f_1^2 \\
\therefore f_2^4 &= f^2 f_1^2 \\
\therefore f_2 &= \sqrt{f \cdot f_1}
\end{aligned} \tag{C.3}$$